R. & M. No. 3013
(17,669)
A.R.C. Technical Report

MINISTRY OF SUPPLY

AERONAUTICAL RESEARCH COUNCIL
REPORTS AND MEMORANDA

Internal Air-Cooling for Turbine Blades
A General Design Survey

By

D. G. AINLEY

LONDON: HER MAJESTY'S STATIONERY OFFICE
1957
PRICE 11s 6d NET

Internal Air-Cooling for Turbine Blades
A General Design Survey

By

D. G. Ainley

Communicated by the Director-General of Scientific Research (Air),
Ministry of Supply

Reports and Memoranda No. 3013*

April, 1955

Summary.—The degree of cooling that might be achieved in gas-turbine blades with simple internal air-cooling is surveyed with a view to pin-pointing the essential requirements for effective cooling with small quantities of cooling air. A shape parameter Z (defined as $(S_c/c)^{1\cdot 2}/(A_c/c^2))$ is derived which forms a useful figure of merit for comparing the relative efficiencies of various cooling passage configurations. To secure maximum economy in total cooling air in blades with a given cooling passage configuration, it is desirable that the turbine-blade rows should be designed with high pitch/chord ratios and low relative gas outlet angles (measured from axial direction). These requirements may run counter to those for high turbine-expansion efficiency and in practice some compromise must be sought to give optimum overall efficiency.

It is shown that efficient blade cooling becomes progressively more difficult at lower values of turbine-flow Reynolds numbers, and cooling systems should be designed to give adequate cooling at the lowest operating Reynolds numbers since this represents the most onerous condition.

The potentialities of blades with laminar-cooling and turbulent-cooling flow in the cooling passages are compared. Although laminar-cooling flow might enable better cooling at low Reynolds numbers to be achieved, turbulent-cooling flow is generally to be preferred since this (*a*) permits more consistent cooling over a wide range of Reynolds number in a simple air-cooled engine and (*b*) presents a simpler blade manufacturing problem.

1. *Introduction.*—The design and the theoretical prediction of the cooling performance of internally air-cooled turbine blades is far from being an exact science. The large number of both aerodynamic and geometric variables which might influence the cooling characteristics create a considerable degree of complexity in the problem. A natural consequence of this is a tendency at present for engine designers to develop cooled blades almost entirely by *ad hoc* experiment and test.

The object of the present report is to show that the influence of quite a large number of the geometric and aerodynamic variables affecting the cooling performance can, in fact, be predicted to a fairly useful degree of accuracy and without a great deal of effort. In particular it is possible to define many of the essential requirements for high efficiency of cooling. This in turn should enable designers to be more highly selective in the types of cooled blade chosen for serious experimental development.

The approximate theory developed in the report is restricted to blades which are internally cooled by forcing air through a number of passages of constant cross-section shape, passing span-wise from root to tip. Such blades have been shown to have attractive cooling characteristics (Ref. 1), and are most amenable to analytical investigation at the present time. Nevertheless, many of the conclusions reached are equally applicable to more complex cooling arrangements and in a qualitative sense the above restriction is not highly critical.

* N.G.T.E. Note NT. 174, received 9th June, 1955.

2. *General Outline of the Problem of Blade Cooling.*—If a blade is somehow maintained at a temperature lower than the effective temperature of the gas flowing over it then heat is transferred from the gas to the blade by a process of forced convection. Some heat may also be transmitted to or from the blade surface by thermal radiation, the quantity depending upon the temperatures, shapes, sizes, and emissivities of the blade surface and its surroundings. Lastly, heat may also be carried to or from the blade by conduction through the blade material.

Usually the forced convective-heat transfer predominates and this is the only heat flow considered in detail in this report. In a turbine in which both the blades and the adjacent ducting all operate at temperatures in the region of about, say, 800 deg C, heat transfer by radiation will be relatively small. Since this condition will probably represent common practice in the near future the possible effects of radiation have not been considered here in detail. It is worth noting, nevertheless, that appreciable radiation effects can arise in certain instances, a few of which are listed below:

(*a*) In turbine stages incorporating uncooled ducts or blades (possibly refractory) adjacent to cooled blades

(*b*) In cascade tunnels when the adjacent ducting and, in particular, adjacent dummy blades are either uncooled on the one hand or cooled to a relatively low value on the other. If the temperatures of surfaces adjacent to a cooled blade are very high then, of course, the effect of radiation will become most marked when the cooled blade temperature is low, and vice versa

(*c*) Radiation heating or cooling will become progressively more marked as the operating temperatures increase (since radiant-heat transfer varies generally in proportion to T^4) and also as the gas-flow Reynolds number decreases (since convective-heat transfer to blades will decrease roughly in proportion to $Re_g^{0 \cdot 7}$).

Usually it is difficult to make a reliable assessment of the effects of radiation, when they arise, due to the complicated shape of the radiating and receiving surfaces involved and also due to the variable nature of the emissivities of various materials with surface physical conditions. Ref. 2 (Brown, 1951), nevertheless, gives a useful and simple theoretical treatment of the radiation-heat transfer occurring between cooled rotor-blade rows and adjacent uncooled (refractory) nozzle-blade rows.

Heat transfer from the blade might be expected by conduction through the blade metal to the cooler blade roots and discs. The conductivities of normal heat resistant materials and spanwise blade temperature gradients are sufficiently low, however, for the net heat conducted in a spanwise direction to be neglected in comparison to convective-heat flow, over normal ranges of gas-flow Reynolds number. Heat transfer by conduction is then found to be of significant importance only when estimating chordwise variation of blade temperature.

Returning to forced convection-heat flow it is clear that the first essential requirement for assessing the performance of a cooled blade is an understanding of the dominant factors affecting the values of gas to blade heat-transfer coefficients (referred to generally as 'external' heat-transfer coefficients). This is discussed in some detail in section 3 later.

To maintain an internally air-cooled blade at a low temperature the heat transferred from the gas to the blade must be picked up by forced convection in the cooling passages and carried away by the cooling air. To provide good cooling in a gas-turbine blade the essential requirements are clearly:

(*a*) a high internal heat-transfer coefficient

(*b*) a large internal cooled surface area

(*c*) as small a quantity of cooling flow as possible, in order to minimise losses in overall engine performance caused by bleeding cooling air away from the engine compressor (*d*) the cooling air pressure drop in passing through the blade should be within the limits set by the particular engine cycle if cooling air pressures are nowhere to exceed the engine-compressor delivery pressure.

Regarding requirement (*c*) some compromise in cooling flow quantity may be necessary since the smaller the cooling flow then the greater will be the rate at which the cooling flow is heated as it passes through a blade, and the greater, therefore, will be the rate at which the blade temperature increases from root to tip.

The number of variables (both geometric and aerodynamic) affecting the internal heat transfer are large and it is clearly essential to have an understanding of these factors, and also those affecting the cooling air pressure loss. These are discussed in detail in sections 4 and 6.

3. *External Heat-Transfer Coefficients*.—The well-established practice of expressing heat-transfer coefficients non-dimensionally in terms of Nusselt numbers is adhered to throughout the present report. Local heat-transfer coefficients at any point on a blade are expressed by a local Nusselt number, Nu_g, defined by $h_g c/\lambda_g$ (*see* Appendix I for notation). The mean value of heat-transfer coefficient on a blade is expressed by a mean Nusselt number, $\bar{N}u_g$, defined by $\bar{h}_g c/\lambda_g$.

It is demonstrated in standard text books on heat transfer (*e.g.*, Refs. 3 and 4) that when temperature variations in the gas-flow boundary layer are small, Nu at any point on a surface is a function only of Reynolds number Re, Prandtl number Pr, and the surface shape. In practice, however, the temperature variations through the boundary layers on cooled turbine blades are frequently large. Many experimentors have attempted to preserve a simple unique relationship between $\bar{N}u_g$, Re_g, and Pr_g for any given blade shape by defining the various gas properties (viscosity, conductivity and density) at some empirically determined intermediate temperature between the gas temperature and the mean blade-surface temperature. Such a process may be convenient for purposes of analysis of experimental data but the complicated definitions of Nusselt number and Reynolds number which result make it very tedious for a turbine designer to apply such data in reverse to the problem of designing a cooled blade and predicting its performance. A simple alternative is to adhere to the practice of always defining gas viscosity and conductivity at gas total temperature and introducing a correction (generally small) which is dependent upon the ratio of gas absolute temperature to mean blade absolute temperature ($T_g/\bar{T}_b$). This is found to be very convenient in practice since the correction for $T_g/\bar{T}_b$ is generally less than 10 per cent and for many approximate calculations it might be ignored.

For heat-transfer calculations the gas temperature adopted should be the 'effective' gas temperature, *i.e.*, the temperature the blades would assume if there was no cooling and no loss of heat by conduction or radiation. This temperature may be approximately defined by:

$$T_g = T_{g(\text{total})}\left[1 - 0\cdot 15\left\{\frac{\frac{\gamma - 1}{2}\bar{M}^2}{1 + \frac{\gamma - 1}{2}\bar{M}^2}\right\}\right].$$

where $\bar{M}$ is the mean Mach number of the flow around the blade profile. For low Mach numbers (less than about $0\cdot 5$) a negligible error is introduced if T_g is assumed to be equal to the gas total temperature, measured relative to the blade.

A further simplification arises in that over a wide range of air temperatures applicable to gas-turbine practice the Prandtl number remains substantially constant (a value of $0\cdot 71$ is assumed throughout) so that Prandtl number can be ignored as an operative variable in the present problem.

Fig. 1 illustrates the variation of local Nusselt number around one typical turbine-blade profile (two-dimensional flow). This distribution is calculated using Squire's method (Ref. 5). The good general agreement occurring between theory and experiment is demonstrated in Ref. 6.

It will be observed that at the leading edge, where the boundary layer is thin and laminar, the local heat-transfer coefficient is large and that it decreases rapidly around the profile as the boundary layer thickens. A rapid increase may be anticipated at the point where the boundary layer changes from laminar to turbulent flow. The magnitude of the high local value of heat transfer at the leading edge is largely dependent upon the leading edge radius. The larger the radius the smaller the local heat-transfer coefficient at the stagnation point will become. This is illustrated in Fig. 1 where it is demonstrated that if the leading-edge radius is increased from 3 per cent to 6 per cent of the chord the local heat-transfer coefficient is decreased by roughly 30 per cent.

The calculated variation of the mean value of Nusselt number, $\bar{Nu}_g$, with gas-flow Reynolds number, Re_g, is illustrated in Fig. 2 for three types of turbine blade with transition occurring at various arbitrarily assumed positions on the blades. It is of particular interest to note that although the shapes and velocity distributions around the three blade types vary appreciably, the relationships between Nu_g and Re_g for each blade, when transition occurs at the same relative positions on all blades, are to a first approximation not markedly different. It is clear, in fact, that the position of the transition regions (or, more significantly, the relative proportion of the blade surface over which the boundary layer is turbulent) has a dominating influence on the mean value of heat-transfer coefficient.

In practice, of course, it is the nature of the pressure distribution over the surface which may largely govern the position of the transition regions and high reaction (*e.g.*, nozzle) blades may usually be expected to have a much larger area of laminar boundary layer than low reaction (*e.g.*, impulse) blades. Now as the proportion of the blade surface over which the boundary-layer flow is turbulent increases the value of $\bar{Nu}_g$ at any given Reynolds number increases. Furthermore, $\bar{Nu}_g$ varies in proportion with $(Re_g)^x$ in such a way that the exponent x increases gradually from a value of $0 \cdot 5$ for a fully laminar boundary layer to $0 \cdot 8$ for a fully turbulent boundary layer. Thus it may be anticipated from the foregoing considerations that at a given value of Reynolds number the value of the mean Nusselt number and the Reynolds-number exponent x will increase as the blade reaction decreases.

This is broadly substantiated in Fig. 3, which attempts to give an approximate correlation of $\bar{Nu}_g$ and x for a fairly wide variety of turbine blades (as determined from National Gas Turbine Establishment and other published experimental data) at a fixed reference Reynolds number of 2×10^5. In deriving this relationship it was assumed that for any given blade:

$$\bar{Nu}_g = \bar{Nu}_g{}^* \left(\frac{Re_g}{2 \times 10^5}\right)^x \left(\frac{T_g}{\bar{T}_b}\right)^y, \quad \ldots \quad (1)$$

where $\bar{Nu}_g{}^*$ is the value of $\bar{Nu}_g$ when $Re_g = 2 \times 10^5$ and $T_g/\bar{T}_b \rightarrow 1 \cdot 0$. It was assumed that $y = 0 \cdot 14(Re_g/2 \times 10^5)^{-0 \cdot 4}$, this value being derived from unpublished work at N.G.T.E., and values for $\bar{Nu}_g{}^*$ and x were then derived for the various blade shapes from the published experimental data.

The relationship suggested in Fig. 3 can only be regarded as approximate; in fact it implicitly presupposes that for a wide variety of turbine-blade shapes the proportion of surface over which the flow is turbulent (at a Reynolds number of 2×10^5) is to a first approximation closely related with the ratio of blade inlet angle to gas outlet angle. Although this may be nearly true for a related family of blade shapes built up, say, from a standard aerofoil section onto camber-lines of standard shape and all tested in a tunnel of constant turbulence, it is hardly likely to be very accurate for the wide variety of unrelated blade shapes and varying turbulence conditions encountered in general turbine engineering practice. Even so, the experimental values of $\bar{Nu}_g{}^*$ and x plotted in Fig. 3, which come from a wide variety of sources (Refs. 6, 7, 8, 9, and 10) in which the blade profile shapes are quite unrelated and the measurement techniques differed greatly, do not show a particularly excessive scatter. This relationship should, therefore, be useful for immediate turbine engineering purposes where a very high accuracy in the value of $\bar{Nu}_g{}^*$ is not critical.

It will be noted that Fig. 3 suggests a higher level of values of $\bar{N}u_g$ and x for blades in turbines (*see* Ref. 1) than for those fitted in cascade tunnels; this reflecting the larger scale of turbulence and unsteady flow anticipated in a turbine as compared with the flow usually present in a typical cascade tunnel.

The value of the temperature-ratio exponent, y, in equation (1) is perhaps the greatest unknown at the time of writing. However, the sparse evidence at present available suggests that its value for turbine-blade profiles is generally less than 0·2, and since values of $T_g/\bar{T}_b$ will rarely exceed 1·5 in the foreseeable future, the effect of the temperature-ratio correction is likely to be relatively small.

4. *Heat Transfer in Straight Cooling Passages of Uniform Cross-Section*.—4.1. *Turbulent Flow*.— This problem has been explored comprehensively by the National Advisory Committee for Aeronautics (U.S.A.) and other investigators for turbulent flow in passages of various cross-sectional shapes and length/diameter ratio, over a wide range of internal-flow Reynolds number, Re_c, and air to wall temperature ratio, $\bar{T}_c/\bar{T}_b$. The results are presented in various forms in Refs. 11 and 12. However, following the form adopted in section 3, it is convenient to express all cooling-flow properties at mean bulk cooling temperature $\bar{T}_c$, and to add a correction factor for the ratio of mean cooling air temperature to mean blade temperature, $\bar{T}_c/\bar{T}_b$. The following relationship for $\bar{N}u_c$ and the governing parameters may then be deduced from Ref. 11:

$$\bar{N}u_c = 0\cdot034(L/D_e)^{-0\cdot1}(Pr_c)^{0\cdot4}(\bar{R}e_c)^{0\cdot8}(\bar{T}_c/\bar{T}_b)^{0\cdot55}. \qquad (2)$$

For $Pr_c = 0\cdot71$ and $L/D_e = 50$, equation (2) reduces to:

$$\bar{N}u_c = 0\cdot020(\bar{R}e_c)^{0\cdot8}(\bar{T}/_c\bar{T}_b)^{0\cdot55}. \qquad (3)$$

Since the constant varies only very slowly with L/D_e the simpler equation (3) can be used with little error over a range of L/D_e of about 30 to 100.

Heat transfer with turbulent flow inside stationary tubes and passages of constant cross-sectional area is perhaps the most fully explored problem in the field of heat transfer, and equations (2) and (3) have been shown to hold to a good degree of accuracy down to mean cooling flow Reynolds numbers of about 8,000. Between $Re_e = 8{,}000$ and the critical value for turbulent flow (about 2,300), test data suggests that the equations will over-estimate the heat transfer, the maximum error being about 30 per cent at $Re_c \simeq 2{,}300$.

It is probable that the equations are almost equally good for passages in rapidly rotating rotor blades although some slight influence might be anticipated due to (*a*) the secondary flow induced in the air flow by Coriolis forces and (*b*) the larger values of Grashof number (associated with the high relative '*g*'). The secondary flow effect is likely to be the major one and arises due to the fact that the air passing through a rotor blade actually follows a curved path (relative to the turbine casing). It might consequently be anticipated that the effect on heat transfer would to a first approximation be similar to that occurring with flow in a curved pipe. The ratio of passage diameter to the effective radius of bend would be very small in a practical instance, however, and data quoted in Refs. 3 and 4 for heat transfer in curved pipes suggests that mean heat-transfer coefficients would be increased by an amount only of the order of 1 per cent.

4.2. *Laminar Flow*.—Heat transfer for laminar flow of gases in tubes has not been explored experimentally nearly so widely as for turbulent flow and relationships between mean Nusselt, Reynolds, and Prandtl numbers and length/diameter ratio suggested by different investigators (Refs. 3. 4, and 13) vary considerably in their form. A relationship suggested by McAdams (Ref. 4) is preferred for the present investigation, this being:

$$\bar{N}u_c = 1\cdot86\left(\frac{\bar{R}e_cPr_c}{L/D_e}\right)^{0\cdot333}\left(\frac{\bar{\mu}_c}{\bar{\mu}_b}\right)^{0\cdot14}.$$

Since, for air, to a first approximation $\mu \propto T^{0\cdot62}$ over a representative temperature range (500–1,500 deg K.) and $Pr = 0\cdot71$ this equation may be rewritten as:

$$\bar{N}u_c = 1\cdot66\left(\frac{\bar{R}e_c}{L/D_e}\right)^{0\cdot333}\left(\frac{\bar{T}_c}{\bar{T}_b}\right)^{0\cdot087} \quad \ldots \quad (4)$$

$$\simeq 1\cdot66\left(\frac{Re_c}{L/D_e}\right)^{0\cdot333}, \quad \ldots \quad (4a)$$

since $(\bar{T}_c/\bar{T}_b)^{0\cdot087} \simeq 1\cdot0$.

Values of $\bar{N}u_c$ derived from this equation are found to agree reasonably well with alternative empirical formulae, quoted in Refs. 3 and 13, over a range of $Re_c/(L/D_e)$ of 6 to 20.

5. *General Equations for Calculating the Mean Blade Temperatures of Simple Internally Air-cooled Turbine Blades (Turbulent-cooling Flow)*.—The cooling characteristics of a blade over a range of conditions will depend upon whether the cooling flow in the passages is turbulent or laminar. For reasons discussed in section 8 later, however, a turbulent-cooling flow is generally to be preferred. For this reason the bulk of the present report is devoted to blade cooling with turbulent flow, discussion of cooling with laminar flow being confined to section 8.

By employing equations (1) and (3) it is possible to derive a group of equations defining the mean blade temperatures of simple internally air-cooled turbine blades in terms of the several design parameters at the disposal of a designer.

As already mentioned in section 1, the analysis is confined to blades cooled by passing cool air spanwise from root to tip through smooth internal passages having arbitrary size and cross-sectional shape but uniform throughout their length. Furthermore, at any selected spanwise position only the chordwise mean of temperature is estimated. The more difficult problem of assessing the chordwise variation of temperature at any given spanwise condition is outside the scope of the present report.

The full derivation of the equations is given in Appendix I, which in addition contains an outline of a simple recommended procedure for solving the equations and also gives an approximate method for allowing for the heat picked up by the cooling air within the root of a blade.

At any spanwise position along the blade (defined by a value of l/L) the chordwise mean of blade temperature is given approximately by (*see* Appendix I for notation):

$$\frac{T_b - T_{cr}}{T_g - T_{cr}} = 1 - \frac{\bar{X}}{1 + \bar{X}} e^{-\bar{K}} \quad \ldots \quad (5)$$

where

$$\bar{X} = \frac{0\cdot0066}{k}\left(\frac{s}{c}\frac{L}{c}\cos\bar{\alpha}_2\right)^{0\cdot8} Z\phi^{0\cdot8} Re_g^{\,0\cdot8-x}\left(\frac{T_c}{T_g}\right)^{0\cdot824}\left(\frac{T_g}{T_b}\right)^{0\cdot55-y} \quad \ldots \quad (6)$$

$$\bar{K} = \frac{3\cdot24k}{\phi\frac{s}{c}\cos\bar{\alpha}_2 Re_g^{\,1-x}}\,\frac{\bar{X}}{(1+\bar{X})}\,\frac{l}{L}\left\{\left(\frac{T_g}{T_b}\right)^{y}\left(\frac{T_g}{T_c}\right)^{0\cdot15}\right\}. \quad \ldots \quad (7)$$

The bulk cooling air temperature at any spanwise position is given by:

$$\frac{T_c - T_{cr}}{T_g - T_{cr}} = 1 - e^{-\bar{K}}. \quad \ldots \quad (8)$$

The temperatures T_b and T_c in the above equations refer to the chordwise mean values of T_b and T_c at the spanwise section considered.

Inspection of the above equations will reveal that for selected values of cooling-flow ratio, gas-flow Reynolds number, and ratio of gas temperature to inlet cooling air temperature the blade temperature is influenced by the external blade geometrical parameters $\bar{\alpha}_2$, $\beta_1/\bar{\alpha}_2$, $\bar{s}/c$, and L/c, and by a single internal passage-shape parameter, Z, defined as $(S_c/c)^{1\cdot 2}/(A_c/c^2)$.

6. *Pressure Losses in Blade Cooling Passages.*—In passing through the cooling passage of a turbine blade the total and static pressures of the cooling air will be influenced by (*a*) the frictional losses, (*b*) the continuous addition of heat to the cooling air as it passes along the passage and (*c*) the centrifugal force on the cooling air if passing through a rotor blade.

For simple one-dimensional flow in a passage of uniform cross-sectional area the change in total pressure over an element of passage length, δl, may be expressed (Ref. 14) as:

$$\frac{\delta P_c}{P_c} = -\frac{\gamma M_c^2}{2}\frac{\delta T_c}{T_c} - \frac{\gamma M_c^2}{2} 4f\frac{\delta l}{D_e} + \frac{r\omega^2}{Rt_c}\,\delta l \,. \qquad \ldots \quad \ldots \quad \ldots \quad \ldots \qquad (9)$$

When the cooling characteristics of a blade are known so that local values of T_c and Re_c are determined at all points along the passage length then the total pressure losses may be determined by step by step integration of equation (9). A useful method for carrying out such computations is described in Ref. 15. Suitable values of friction coefficient f, may be determined from the data in Refs. 15 or 11.

Although this method must be adopted in practice if a reasonably accurate estimate of the losses in a specific blade is required it is possible to demonstrate broadly the pressure-loss characteristics of cooled blades by the use of simpler approximate formulae.

In a cooled engine it is supposed that the cooling air will be extracted from the main engine compressor and the maximum pressure drop available for forcing cooling air through the cooling passages of any particular row of turbine blades will depend upon the engine design and operating conditions. To a good first approximation this available pressure drop, for a wide range of operating conditions, will be proportional to some fixed multiple of the relative outlet dynamic head of the main gas stream emerging from the row of blades considered (the actual value of this multiple depending upon the particular engine design).

It is convenient, therefore, to express the cooling-air pressure drop in a cooled blade under any given set of operating conditions as a ratio of the relative gas-outlet dynamic pressure.

Simple approximate equations for this pressure-drop coefficient, expressed in terms of convenient parameters such as cooling-flow ratio, aspect ratio, etc., are derived in Appendix II. For turbulent-cooling flow the final equation is:

$$\frac{P_{c\,\text{entry}} - p_{c\,\text{exit}}}{(\frac{1}{2}\rho_g V_g^2)_{\text{outlet}}} = \frac{0\cdot 158\left(\dfrac{\bar{T}_c}{T_g}\right)^{1\cdot 155}\left(1+\dfrac{\bar{T}_b}{\bar{T}_c}\right)\left(\phi\dfrac{sL}{A_c}\cos\bar{\alpha}_2\right)^{1\cdot 75}\dfrac{L^*}{D_e}}{\left(\dfrac{D_e}{c}\right)^{0\cdot 25}(Re_g)^{0\cdot 25}}$$

$$+\left(\phi\frac{sL}{A_c}\cos\bar{\alpha}_2\right)^2\left(\frac{T_{c\,\text{tip}}}{T_g}\right)$$

$$-2\left(\frac{T_g}{\bar{T}_c}\right)\left(\frac{\bar{U}}{V_g}\right)^2\frac{L^*}{\bar{r}}\,. \quad \ldots \quad \ldots \quad \ldots \quad \ldots \quad \ldots \quad \ldots \quad \ldots \qquad (10)$$

The first term on the right-hand side of the equation is the combined loss of total pressure due to friction and heat addition; the second term is the cooling-air dynamic head at the point of discharge from the blade tip (assumed totally lost); the third term applies only to rotor blades and is the rise in total pressure along the blade passage caused by centrifugal compression.

A similar type of equation may also be derived for laminar-cooling flow, namely:

$$\frac{P_{c\,\text{entry}} - p_{c\,\text{exit}}}{(\frac{1}{2}\rho_g V_g^{\,2})_{\text{exit}}} = \frac{32\left(\frac{\bar{T}_c}{T_g}\right)^{1\cdot 62}\left(\frac{\bar{T}_b}{\bar{T}_c}\right)^{0\cdot 45}\left(1+\frac{\bar{T}_b}{\bar{T}_c}\right)\left(\phi\,\frac{sL}{A_c}\cos\bar{\alpha}_2\right)\frac{L^*}{D_e}}{\left(\frac{D_e}{e}\right) Re_g}$$

$$+\left(\phi\,\frac{sL}{A_c}\cos\bar{\alpha}_2\right)^2\left(\frac{T_{c\,\text{tip}}}{T_g}\right)$$

$$-2\left(\frac{T_g}{\bar{T}_c}\right)\left(\frac{\bar{U}}{V_g}\right)^2\frac{L^*}{\bar{r}} \quad \ldots \qquad (11)$$

Strictly speaking these approximate equations only hold true when the cooling and main gas-flow Mach numbers are small. Nevertheless they serve well to demonstrate the relative influence of various blade-design parameters on the resultant pressure-drop coefficient.

Three points of some importance may be noted at this juncture:

(*a*) For a blade of pre-fixed external geometry and operating conditions the pressure-drop coefficient is uniquely determined by A_c and D_e, which in turn are uniquely determined by Z, D_e/c, and c. Thus, differing cooling-passage configurations will have similar pressure-drop characteristics if the values of Z and D_e/c are the same

(*b*) For a well-cooled blade the loss due to friction and heat addition (the first terms on the right-hand side of equations (10) and (11)) predominates over the remaining component losses

(*c*) Bearing point (*b*) in mind it will be seen that for a fixed overall pressure drop, $\phi \propto Re_g^{(0\cdot 25/1\cdot 75)} \propto Re_g^{0\cdot 14}$ when the cooling flow is turbulent, and $\phi \propto Re_g$ when the flow is laminar.

7. *Examination of the Individual Influence of Each of the Aerodynamic and Geometric Parameters Governing the Amount of Cooling.*—The technique adopted in this section is to select arbitrarily a 'datum' set of values for the parameters occurring in equations (5), (6) and (7) (section 5), these defining a 'typical' turbine blade. The blade relative temperature, $T_b - T_{cr}/T_g - T_{cr}$, on this blade at a spanwise position of $l/L = 0\cdot 6$ is calculated and the value of each parameter is then varied, one at a time, and the resulting variation of blade relative temperarure (at $l/L = 0\cdot 6$) noted.

The typical values arbitrarily assumed for the 'datum' blade are as follows:

Outlet gas angle	=	$\bar{\alpha}_2$	=	60 deg	
Inlet blade angle	=	β_1	=	0 deg	
Pitch/chord	=	s/c	=	$0\cdot 75$	
Aspect ratio	=	L/c	=	$2\cdot 0$	
Gas-flow Reynolds number	=	Re_g	=	2×10^5	
Mean Nusselt number	=	$\bar{N}u_g^*$	=	400	Values appropriate to 'turbine' blade
Reynolds number exponent	=	x	=	$0\cdot 65$	($\beta_1/\bar{\alpha}_2 = 0$) from Fig. 3.
Cooling-flow ratio	=	ϕ	=	$0\cdot 015$	
Passage-shape parameter	=	Z	=	200	
Temperature ratio	=	T_g/T_{cr}	$\to$	$1\cdot 0$	

These conditions lead to a blade having a mean blade relative temperature, $T_b - T_{cr}/T_g - T_{cr}$, varying from 0·37 at the root ($l/L = 0$) to 0·69 at the tip ($l/L = 1 \cdot 0$), as shown in Fig. 4. At the selected reference position along the span ($l/L = 0 \cdot 6$) the mean blade relative temperature is 0·59.

7.1. *Influence of Cooling-Flow Ratio and the Passage-Shape Parameter, Z.*—The effect of varying the cooling-flow ratio ϕ and the passage-shape parameter Z on the mean blade relative temperature at $l/L = 0 \cdot 6$ is illustrated jointly in Figs. 5a and 5b. The spanwise variation of blade temperature for a few selected values of ϕ and Z is shown in Fig. 6. From these figures the following points may be noted:

(*a*) When the cooling-flow ratio is increased the blade relative temperature decreases, but the rate of temperature decrease with increase of flow falls away as the cooling-flow ratio increases.

(*b*) For a selected value of cooling-flow ratio the blade temperatures decrease as the passage-shape parameter Z increases. The blade temperature varies fairly rapidly with Z when Z is small, but becomes progressively less sensitive to changes in Z when Z is large.

(*c*) As Z increases the spanwise temperature variations also increase. This is due, of course, to the fact that as Z increases the rate at which heat is transferred to the cooling air per unit blade height is also increased and hence the temperature rise of the cooling air as it passes through the blade is increased.

In general, values of Z in excess of about 150 are required for reasonably good cooling, although the benefits to be gained by increasing Z beyond about 250 are relatively small. In practice, caution is required when designing for high values of Z, to ensure that the cooling-flow Reynolds number does not fall below the critical value for turbulent flow. This point is discussed more fully later in the report.

Strictly the analysis in Appendix I and equations (5), (6) and (7) is only correct when the internal cooling-passage configuration consists of a number of passages of equal size and shape. In this instance the passage-shape parameter, Z, may be expressed as follows :

$$Z = (S_c/c)^{1 \cdot 2}/(A_c/c^2) = 5 \cdot 03(\psi n)^{0 \cdot 2}/(D_e/c)^{0 \cdot 8}, \quad \ldots \quad (12)$$

where n = number of cooling passages

D_e = hydraulic diameter of cooling passages

ψ = a shape factor defined by $S_c'/\pi D_e$

S_c' = periphery of one cooling passage = S_c/n .

The shape factor, ψ, has a minimum value of unity for passages of circular cross-section and higher values for passages of other cross-section. Some typical values are listed below:

Passage shape	ψ
Circular	1·0
Square	1·272
Equilateral triangle	1·652
5 : 1 rectangle	2·29
10 : 1 rectangle	3·85
5 : 1 ellipse	2·24
10 : 1 ellipse	4·17

Clearly, from equation (12), the essential requirements for a high value of Z are (*a*) a small value for D_e/c and (*b*) a large value for ψn. An important point concerning passage cross-sectional shape is at once apparent. If values of Z and D_e/c are pre-selected to give good cooling and low cooling air-pressure drop (it was shown in section 6 that the pressure-drop characteristics are determined by Z and D_c/c) then the actual number of passages required is inversely proportional to the shape factor ψ. In particular, the choice of simple circular passages requires a maximum number of holes whereas if passages of, say, rectangular or elliptical cross-section having an axis ratio of 10 : 1 are employed, the number of passages required is reduced to roughly one quarter of the maximum. This effect of passage shape is illustrated diagrammatically in Fig. 7, which shows three alternative patterns of cooling passage which should theoretically give similar cooling and pressure-drop characteristics (*i.e.*, similar values of Z and D_e/c).

When the passages in a given blade are not all of the same size and shape the direct use of equations (5), (6) and (7) will tend to over-estimate the degree of cooling achievable. This happens since in practice a greater weight of cooling air will pass through the holes which are larger than average size than through the holes that are smaller than average, so that the 'effective' value of Z will be rather less than the overall value estimated from $(S_c/c)^{1\cdot2}/(A_c/c^2)$. It is shown in Appendix IV that the 'effective' value of Z may be expressed by:

$$Z_{\text{effective}} = \frac{c^{0\cdot8} \sum_{r=1}^{n} \dfrac{S_{cr}^{\ 1\cdot086}}{A_{cr}^{\ 0\cdot036}}}{\left\{ \sum_{r=1}^{n} \dfrac{A_{cr}^{\ 1\cdot143}}{S_{cr}^{\ 0\cdot143}} \right\}^{0\cdot8}}, \quad \ldots \quad \ldots \quad \ldots \quad \ldots \quad \ldots \quad (13)$$

where the suffix r denotes values ascribed to A_c and S_c in each individual passage.

In deriving the expressions for estimating the degree of cooling, and incidentally the Z factor, it has been assumed that heat is conducted readily to the entire surface of the cooling passages. In some cooling-passage configurations it may happen that the heat flow conducted to some parts of the cooling-passage periphery is 'throttled' (due to long heat flow paths in local parts of the blade, coupled with low metal thermal conductivities). In such instances it may be necessary to multiply the value of Z by a factor, η, analogous to the fin efficiency in the cooling of finned bodies. No rules may be formulated for rapidly assessing an appropriate value for η at the present state of the art, although for the types of passage considered in this report, *e.g.*, Fig. 7, it is improbable that the value of η will be less than about $0\cdot9$. In the present calculations a value of unity is assumed throughout.

7.2. *Influence of Blade External Geometry*.—7.2. (*a*) *Pitch/chord ratio*.—The wider the blade spacing then the fewer will be the number of blades in a row to be cooled and hence, for a given overall value of cooling-flow ratio, the greater will be the quantity of cooling air available for each individual blade. It is to be expected therefore that the degree of cooling achieved in blade row (for a given overall cooling-flow ratio) will be improved by increasing the pitch/chord ratio. This is demonstrated in Fig. 5c. At the same time some increase in the value of D_c/c, ψ, or n (whilst preserving a similar value of Z) would be required to prevent an increase in cooling-air pressure loss. In fact, if no adjustment other than an alteration in spacing were made in a blade row in which the cooling flow was metered by the cooling-air pressure drop in the passages then no change in the degree of cooling would occur, although the cooling-flow ratio would decrease as the spacing were increased.

7.2. (*b*) *Blade aspect ratio*.—The influence of aspect ratio on the degree of cooling of the typical reference blade is shown in Fig. 5e. If the gas-flow Reynolds number remains constant then the degree of cooling improves with increase of aspect ratio, although in the present instance aspect ratios greater than about $2\cdot0$ produce only small improvements in cooling. The underlying reason for this general influence of aspect ratio is, perhaps, not immediately obvious. It may be seen, however, from Appendix I (equation (18)) that the ratio of internal cooling-flow Reynolds number to external gas-flow Reynolds number is proportional to aspect ratio. Thus, for a constant gas-flow Reynolds number the internal cooling-flow Reynolds number increases as the aspect ratio is increased and hence the internal heat-transfer coefficient is also increased, with a consequent reduction in blade temperature.

When selecting a value for aspect ratio in practice the blade height and gas-flow conditions will usually have been pre-determined, with the result that the operating gas-flow Reynolds number will vary in direct proportion with the chord length chosen (i.e., $Re_g \propto c/L$). It will be seen from Fig. 5c that when this is the case the variation of blade relative temperature with aspect ratio is much reduced and that there is in fact an optimum value of the aspect ratio for maximum cooling. The optimum value of aspect ratio for the reference blade is roughly $2 \cdot 0$, although this value will vary slightly for other blade arrangements.

7.2. (*c*) *Influence of gas outlet angle*.—Fig. 5d illustrates the influence of gas outlet angle on blade cooling, all other factors (cooling-flow ratio, cooling-passage configuration, etc.) being fixed. Over the range of outlet angles of 45 deg to 70 deg normally encountered in conventional turbine design the variation of blade temperatures is relatively large, the best cooling being obtained with the lowest outlet angles. The reason for this might be explained as follows. As the outlet angle of a given blade is increased (measured from axial direction) the throat area decreases, with the consequence that the gas mass flow through each blade gas-flow passage also decreases (gas-flow Reynolds number being assumed constant). For a fixed value of cooling-flow ratio the cooling flow per blade will therefore decrease in proportion, with a resulting loss in cooling. It should be noted particularly that the variation of blade temperature shown in Fig. 5d is not associated with any change in mean external Nusselt number consequent upon a change in blade setting or shape as outlet angle is changed. In the example shown it is assumed that $\beta_1/\bar{\alpha}_2$ remains constant (zero in this instance) and, as illustrated in Fig. 3, $\bar{Nu}_g{}^*$ is assumed to remain constant over a wide range of blade outlet angles if the ratio $\beta_1/\bar{\alpha}_2$ is held constant.

The marked influence of blade gas-outlet angle on the cooling efficiency of the blades clearly has a repercussion on the optimum design velocity triangles for a cooled turbine stage. This analysis indicates that to achieve a high degree of cooling with a low cooling-flow ratio it is desirable to achieve the required turbine work output by designing the stages with relatively low gas deflections and a high ratio of gas axial velocity to blade peripheral velocity. Unfortunately, however, it is known that such stage designs may have lower total head efficiencies and may give rise to higher exhaust-duct losses than stages with higher gas deflections and lower gas axial velocities. Any reduction in turbine expansion efficiency due to using low deflection blading must, therefore, be offset against the higher cooling efficiency (or smaller cooling flows) obtained, and in practice some compromise must be struck to give optimum overall engine performance. The optimum blading arrangement is likely to vary somewhat with different engine configurations and at the present stage of knowledge it is unfortunately not possible to give any generalised analysis of this problem.

7.2. (*d*) *Influence of inlet blade angle*.—This is illustrated in Fig. 5f where it is shown that cooling effectiveness is reduced as the inlet blade angle (or, more correctly, the ratio $\beta_1/\bar{\alpha}_2$) is increased. This variation is due entirely to the increase in $\bar{Nu}_g{}^*$ associated with an increase in $\beta_1/\bar{\alpha}_2$ (indicated in Fig. 3), the rise in $\bar{Nu}_g{}^*$ being presumed to be associated with a general increase in the proportion of turbulent boundary layer on the blade surface as the degree of reaction is reduced.

Two curves are plotted in Fig. 5f showing the theoretical blade temperatures resulting from the assumed relationships between $\bar{Nu}_g{}^*$ and $\beta_1/\bar{\alpha}_2$ for (i) blades in an actual turbine stage and (ii) blades in lower turbulence cascade tunnels (*see* section 3). This illustrates the order of magnitude of the difference in actual blade temperatures which might easily occur between blades tested in a cascade tunnel and identical blades tested in an actual turbine stage.

7.3. *Effect of the Ratio of Gas Temperature to Cooling-Air Inlet Temperature*.—The calculations illustrated in Figs. 5 and 6 were made assuming that the actual temperature differences between gas and cooling air were small, *i.e.*, $T_g/T_{cr} \rightarrow 1 \cdot 0$. As the ratio T_g/T_{cr} increases to more practical values of 2 or more then so also will the ratio of gas temperature to mean blade temperature

$(T_g/\bar{T}_b)$ increase, together with the ratio of mean blade temperature to mean cooling air temperature $(\bar{T}_b/\bar{T}_{cr})$. Now it was indicated in section 3 that an increase in $T_g/\bar{T}_b$ causes a slight increase in the external heat-transfer coefficient (at a given Reynolds number, Re_g). Similarly it will be noted from equation (3), section 4.1, that an increase in the ratio $\bar{T}_b/\bar{T}_c$ causes a reduction in the internal heat-transfer coefficient. It may be anticipated from this, therefore, that an increase in the ratio of gas to cooling-air temperature will cause a small increase in the mean blade relative temperature (*i.e.*, reduction in the relative degree of cooling).

This is illustrated for the ' typical ' reference blade in Fig. 8a, where the influence of T_g/T_{cr} on blade relative temperature is estimated for values of cooling-flow ratio of 1 per cent to 2 per cent and cooling passage-shape parameter Z of 100 and 300. The relative degree of cooling lost as a result of increasing the ratio of gas temperature to cooling-air inlet temperature is illustrated more directly in Fig. 8b. In this figure the relative degree of cooling $(T_g - T_b/T_g - T_{cr})$ at each value of T_g/T_{cr} is plotted as a ratio of the relative degree of cooling obtained when $T_g/T_{cr} \rightarrow 1 \cdot 0$ (defined as $(T_g - T_b/T_g - T_{cr})^*$). From this figure it will be seen that the loss in cooling is appreciably lower for high values of passage-shape parameter Z than for low values of Z.

The ratio of gas to cooling-air temperature also has a pronounced effect on the cooling-air pressure-drop characteristics. The pressure-drop coefficient, $\Delta P_c/\frac{1}{2}\rho_g V_g^2$, at any given value of cooling-flow ratio decreases appreciably as the ratio T_g/T_{cr} is increased. The reason for this is simply that an increase in $T_g/\bar{T}_{cr}$ is accompanied by an increase in the ratio of mean cooling air density to main gas-flow density, $\bar{\rho}_c/\rho_g$, and (for constant cooling-flow ratio) by an inversely proportional reduction in the ratio of mean cooling-air velocity to gas-flow velocity, $\bar{V}_c/V_g$. This leads to a reduction in the ratio of mean cooling-flow dynamic head to gas-flow dynamic head $(\frac{1}{2}\bar{\rho}_c\bar{V}_c^2/\frac{1}{2}\rho_g V_g^2)$ and hence to a reduction in pressure-drop coefficient $\Delta P_c/\frac{1}{2}\rho_g V_g^2$, since ΔP_c remains roughly proportional to $\frac{1}{2}\bar{\rho}_c\bar{V}_c^2$. This effect is illustrated in Fig. 9 where the pressure-drop coefficient for the typical blade defined in section 7 (having $Z = 200$ and, in addition, an assumption that $D_c/c = 0 \cdot 025$) is plotted against the cooling-flow ratio for values of $T_g/T_{cr} = 1 \cdot 0$, $2 \cdot 0$, and $3 \cdot 0$. An effect similar to that calculated on Fig. 9 was observed experimentally on an experimental air-cooled turbine reported in Ref. 1.

It is of interest to note that if the available cooling-air pressure-drop coefficient over a turbine blade remains constant over a range of turbine operating conditions (as might be expected, approximately, in an engine) then the cooling-flow ratio will increase as T_g/T_{cr} increases, and this increase in cooling flow will tend to offset, and in fact nearly counterbalance, the reduction in blade relative temperature predicted in Fig. 8 for a constant flow ratio.

7.4. *Influence of Gas-Flow Reynolds Number.*—It was shown in section 3 that the mean external (gas to blade) heat-transfer coefficient decreases with gas-flow Reynolds number in proportion to $(Re_g)^x$, where x will have a value in the region of $0 \cdot 6$ to $0 \cdot 75$ depending upon the blade shape and setting angle. Heat flowing into a cooled blade will, therefore, decrease with decreasing Reynolds number in proportion to $(Re_g)^x$. It was also shown in section 4 that the internal (blade to cooling air) heat transfer decreases as the internal cooling-flow Reynolds number decreases, in proportion to $(\bar{R}e_c)^{0 \cdot 8}$. Now when the cooling-flow ratio and the ratio of gas temperature to cooling-air inlet temperature, T_g/T_{cr}, are held constant the ratio of mean cooling-flow Reynolds number to gas-flow Reynolds number, $\bar{R}e_c/Re_g$ also remains constant. It will be seen therefore that with constant values of cooling-flow ratio and T_g/T_{cr} and decreasing values of Re_g the rate at which heat can be removed from the blade by the cooling air decreases more than the rate at which the heat flowing into the blade decreases. This results in a tendency for the blade relative temperature to increase when the gas-flow Reynolds number Re_g is reduced.

The calculated variation of blade relative temperature with gas-flow Reynolds number for the reference ' datum ' blade is plotted in Fig. 10 for cooling-flow ratios of $0 \cdot 01$ and $0 \cdot 02$ and for values of T_g/T_{cr} of 1.0 and $3 \cdot 0$. It may be seen for example that with $T_g/T_{cr} = 3 \cdot 0$ and a cooling-flow ratio $\phi = 0 \cdot 02$ that the blade relative temperature increases gradually from $0 \cdot 56$ at $Re_g = 6 \times 10^5$ to $0 \cdot 665$ at $Re_g = 6 \times 10^4$. Such an effect is appreciable and may seriously impair the degree of cooling achieved in air-cooled aircraft-engine turbine blades at high altitudes.

It should be noted that the variation in blade relative temperature is primarily dependent upon the value of the Reynolds number exponent x in equation (1) (section 3), and that for low reaction blades having a large proportion of turbulent boundary and values of x in the vicinity of $0 \cdot 75$ the variation of blade temperature with Re_g would be very much less than with high reaction or nozzle blades having lower values of x (about $0 \cdot 6$). At the same time, at any given value of Reynolds number, the actual degree of cooling achieved on the low reaction blades may be less than with the high reaction blades due to the high mean values of heat-transfer coefficient associated with the former (*cf.* Sections 3 and 7.2 (*d*) and Figs. 3 and 5f).

A further important effect associated with reduction of Re_g must be noted. Since the cooling-flow Reynolds number $\bar{R}e_c$ decreases in proportion to Re_g for any given blade design there will occur a critical value of Re_g below which the cooling-flow Reynolds number $\bar{R}e_c$ will be less than the critical value for turbulent flow, the cooling flow then becoming laminar. A decrease of $\bar{R}e_c$ towards and past the critical value (about 2,300) will be accompanied by a fairly rapid decrease of internal heat-transfer coefficient (Ref. 11) which has not been allowed for in the estimations of blade relative temperature, so that in the vicinity of the critical values of Re_g shown in Fig. 10 a sharper increase in blade temperature than that illustrated might be expected. A more realistic picture is probably that illustrated in Fig. 11, which was estimated for the same blade operating at a constant value of cooling-flow ratio of $0 \cdot 015$ and $T_g/T_{cr} \rightarrow 1 \cdot 0$.

If the cooling-flow ratio is controlled by a fixed overall value of the cooling-air pressure-drop coefficient (*see* section 6.0) then the increase in blade temperature with decreasing Reynolds number becomes more severe, particularly if the cooling flow is laminar. This is due to the increase in skin-friction coefficient accompanying a decrease in $\bar{R}e_c$, which causes a reduction in the cooling-flow ratio. This is effect discussed in more detail in section 8.

If it is desired to operate a cooled blade over a wide range of Re_g, with low minimum values, and it is also desired to retain a turbulent flow in the cooling passages under all conditions (as is generally the case) then a difficult compromise may be introduced into the design, as follows. To maintain turbulent flow in smooth cooling passages at low values of gas-flow Reynolds number, Re_g, it is necessary that the ratio $\bar{R}e_c/Re_g$ must be as high as possible. However, for a blade of predetermined external geometry and cooling-flow ratio and having a fixed overall value of the cooling-air pressure-drop coefficient it is found that, approximately:

$$\bar{R}e_c/Re_g \propto 1/Z^{1 \cdot 3} \quad \ldots \quad (14)$$

This implies therefore that a high value of $\bar{R}e_c/Re_g$ is incompatible with a high value of Z, so that some sacrifice in the relative degree of cooling is necessitated if a turbine is required to operate with turbulent cooling flow down to low gas-flow Reynolds numbers. The nature of the compromise is broadly indicated in Fig. 12, where, for the reference blade defined in section 7, the critical value of gas-flow Reynolds number, Re_g, is plotted against the passage-shape parameter Z. It may be noted from both Fig. 12 and Fig. 10 that both a high value of T_g/T_{cr} and a high value of cooling-flow ratio ϕ help to reduce the critical value of Re_g at any given value of Z. The relationships shown on these figures apply, of course, to only one blade and the critical values of Re_g and the variation of blade relative temperature with Re_g will be somewhat different for blades of other scantlings. Nevertheless the scantlings of the reference blade selected in this report are sufficiently typical of high-pressure—stage turbine blades for the figures to give a broadly representative picture. It is also worth emphasising that variations in external geometry leading to good cooling (high pitch/chord ratio, low outlet angle) also help in achieving a low critical gas-flow Reynolds number.

It should, perhaps, be emphasised also that the above paragraphs refer essentially to blades with smooth internal cooling passages. In practice it may always be possible to design blades with internal passages partially filled with small baffles of some description to artificially maintain turbulence at very low Reynolds numbers. A good example of such blades may be 'insert' blades described in Ref. 16.

8. *Air-Cooled Blades with Laminar-Cooling Flow.*—Adopting equation (4*a*) in section 4.2 for the laminar-flow relationship between cooling-flow Nusselt number and cooling-flow Reynolds number it is possible to derive general expressions for blade relative temperature in terms of governing non-dimensional geometric and aerodynamic parameters in the same way as for turbulent-cooling flow (*see* Appendix I). The resulting relationships are:

$$\frac{T_b - T_{cr}}{T_g - T_{cr}} = 1 - \frac{\bar{X}_l}{1 - \bar{X}_l} e^{-\bar{K}_l} \qquad (15)$$

where

$$\bar{X}_l = \left\{\frac{0\cdot456}{k}\left[\frac{s}{c}\cos\bar{\alpha}_2\right]^{0\cdot333} Z_l\right\} \phi^{\,0\cdot033}\, Re_g^{\,0\cdot333-x}\left(\frac{T_c}{T_g}\right)^{0\cdot56}\left(\frac{T_b}{T_g}\right)^{y} \qquad (16)$$

$$Z_l = \left(\frac{S_c}{c}\right)^{1\cdot333} \Big/ \left(\frac{A_c}{c^2}\right)^{0\cdot666} \qquad (17)$$

$$K_l = \left\{\frac{3\cdot24k}{(s/c)\cos\bar{\alpha}_2}\right\}\left(\frac{T_g}{T_b}\right)^{y}\left(\frac{T_g}{T_c}\right)^{0\cdot15}\frac{(l/L)\bar{X}_l}{\phi Re_g^{\,1-x}(1 + X_l)} \qquad (18)$$

With laminar-cooling flow it is seen that the influence of the number, size, and shape of the cooling passages is defined by a cooling-passage-shape parameter Z_l. The parameter Z_l differs from the equivalent parameter Z for turbulent-cooling flow, although it may be shown (Appendix I) that the two are related by the equation:

$$Z_l = \frac{Z^{3\cdot333}(D_e/c)^{2\cdot666}}{40\cdot2} \qquad (19)$$

Taking once again the reference ' datum ' blade of section 7 it is possible to compare the cooling characteristics achieved with both turbulent-cooling and laminar-cooling flow.

It is supposed that the external geometry, cooling-flow ratio, gas-flow Reynolds number, and cooling-air pressure-drop coefficient have been arbitrarily fixed and then the resulting blade relative temperatures, together with the necessary passage sizes and number of passages to meet these requirements, are plotted in Fig. 13 over a large range of Z. This range of Z covers both the laminar and turbulent regimes of cooling flow for two selected values of gas-flow Reynolds number (a ' normal ' value of about 2×10^5, and a ' low ' value of 4×10^4) and a probable transition region between the two is indicated.

From Fig. 13 it may be noted that:

(*a*) the lowest blade temperatures obtained with laminar-cooling flow are less than those obtainable with turbulent-cooling flow, particularly at the lower values of Re_g

(*b*) to achieve a high degree of cooling with laminar flow a very large number of passages of very small diameter are required as compared with those required for turbulent flow. The achievement of laminar flow, therefore, very considerably complicates the manufacturing problem and might also lead to passages more susceptible to fouling and blockage

(*c*) as the value of Re_g decreases the maximum value of the passage-shape parameter Z at which it is possible to maintain turbulent flow in the cooling passages decreases. This point was also emphasised in the previous section 7.4.

A further comparison between laminar and cooling flow is illustrated in Fig. 14a. The variation of blade relative temperature with gas-flow Reynolds number at a constant value of cooling-flow ratio is shown for two blades designed to operate with a laminar and turbulent flow respectively over a range $10^6 > Re_g > 6 \times 10^4$, the cooling-air pressure-drop coefficient for both blades being $1\cdot5$ when $Re_g = 2 \times 10^5$. With the low minimum value of Re_g of 6×10^4 the passage-shape parameter Z is limited to the relatively low value of 100 for the conditions selected and consequently the degree of cooling achieved with turbulent flow is appreciably less than that obtained with the laminar-flow design. On the other hand the laminar-flow design requires a number of cooling passages specified by $\psi n = 640$ having a diameter specified by $D_e/c = 0 \cdot 0103$, whereas the turbulent-flow blade only requires $\psi n = 10$ and $D_e/c = 0 \cdot 042$. Clearly the turbulent-flow blade presents a much simpler manufacturing task.

If the cooling ratio is held constant at all values of Re_g (as in Fig. 14a) the rate of variation of mean blade relative temperature with gas-flow Reynolds number is broadly similar for both designs. In practice, however, it is more probable that in a turbine the cooling-air pressure-drop coefficient will remain substantially constant and the cooling-flow ratio ϕ will vary as Re_g changes. When this happens it is shown in Appendix II that, approximately, for turbulent flow $\phi \propto Re_g^{0 \cdot 14}$ whereas for laminar flow $\phi \propto Re_g$. The much more rapid variation of ϕ with Re_g under these conditions when the flow is laminar will therefore result in a much more rapid variation in blade temperature. This is illustrated in Fig. 14b where the variation in blade relative temperature with Re_g for both the laminar-flow and turbulent-flow blade designs is estimated on the assumption that the cooling-air pressure-drop coefficient remains constant at all values of Re_g. This clearly emphasises the desirability for achieving turbulent-cooling flow in the blade cooling passages if the cooling is to remain reasonably good over a wide operating range of Reynolds number when the cooling flow is metered primarily by the pressure drop in the cooling passages.

9. *Conclusions.*—Simple equations have been derived from which the mean degree of cooling achievable in single-pass internally air-cooled turbine blades may be approximately calculated. Equations are also derived for approximately estimating the cooling-air pressure losses.

By means of these equations it is possible to examine the influence that various design parameters, defining the geometric form and operating conditions of a cooled blade row, have on the cooling characteristics and also to specify the essential requirements for good cooling. Some broad conclusions resulting from such an examination are:

(*a*) When the gas-flow Reynolds number is high (greater than about 10^5) a high degree of cooling (mean blade relative temperature $< 0 \cdot 6$) may be achieved with internal cooling-passage configurations giving either laminar-cooling or turbulent-cooling flow. Turbulent-cooling flow is generally preferable, however, since (i) a relatively small number of cooling passages of relatively large diameter are required as compared with those necessary to achieve laminar flow, and (ii) when the cooling flow is metered primarily by the cooling-air pressure drop through the blades the cooling-flow ratio varies only slowly with changes in gas-flow Reynolds number (such as may occur when an aircraft engine operated over a range of altitudes) whereas with laminar flow the cooling-flow ratio will vary roughly in nearly direct proportion to the Reynolds number.

(*b*) At low gas-flow Reynolds numbers, with smooth internal cooling passages, the degree of cooling achievable with turbulent flow is less than that achievable with laminar flow. Better cooling with turbulent flow at low gas-flow Reynolds numbers might however be achieved if some means are employed for artificially creating and maintaining turbulent flow in fine cooling passages.

(*c*) All forms of internally air-cooled blade, when operated at a constant value of cooling-flow ratio, are likely to suffer some loss in the degree of cooling when gas-flow Reynolds number decreases. High reaction blades are likely to show greater variations of cooling with change in Reynolds number than low reaction blades. The above reduction of cooling with decrease in Reynolds number is likely to be accentuated further if the cooling flow is metered primarily by the cooling-air pressure drop within the cooling passages, since with such a system the cooling-flow ratio will tend to decrease with reducing Reynolds number. This decrease in cooling-flow ratio and the resulting loss of cooling may become very serious if the cooling flow becomes laminar. It would seem important, therefore, that an air-cooled blade should be designed to satisfy the required cooling performance at the lowest operating Reynolds number in any specified engine since this clearly presents the most onerous condition.

(*d*) When radiation and conduction effects are negligible the non-dimensional operating parameters defining the relative non-dimensional blade temperature $[(T_b - T_{cr})/(T_g - T_{cr})]$ in a cooled blade row are (i) the cooling-flow ratio ϕ, (ii) the gas-flow Reynolds number, Re_g, and (iii) the ratio of gas temperature to cooling-air inlet temperature T_g/T_{cr}. These remarks presuppose that Prandtl number remains substantially constant over a wide range of gas temperatures and that to eliminate the influence of gas-flow Mach number the gas temperature is the 'effective' value defined, approximately, as static temperature + 0·85 of the mean kinetic temperature.

(*e*) To achieve good cooling with maximum economy of cooling air it is desirable that the blades should have (i) low gas-outlet angles (measured from the axial direction) and (ii) high pitch/chord ratios. Requirements (i) and (ii) are not entirely compatible with the desirable stage design requirements for high turbine-expansion efficiency, and some compromise between high turbine efficiency on the one hand and low quantity of cooling flow on the other must be sought to achieve optimum overall performance in any specified cooled engine.

(*f*) With turbulent-cooling flow a useful figure of merit for comparing the effectiveness of various cooling passage configurations is the cooling-passage shape parameter Z, defined by the ratio $(S_c/c)^{1\cdot 2}/(A_c/c^2)$. In general Z should be made as high as possible for good cooling, although improvements in cooling performance become relatively small when $Z > 250$.

(*g*) The cooling-air pressure-drop characteristics of a given cooled blade are dependent upon the cooling passage-shape parameter Z, and the hydraulic mean diameter of the passages, D_e. In a blade of fixed external design then cooling passage configurations having similar values of D_e and Z will have similar pressure-drop characteristics. For preselected values of D_e and Z the number of passages is a maximum when the passages are of circular cross-section. For other cross-sectional shapes the number of passages required varies inversely as the ratio of (hole periphery)$/\pi D_e$. Thus, for example, to achieve a certain degree of cooling for a predetermined cooling-flow ratio and cooling-air pressure drop the use of highly elliptical or rectangular shaped passages would require a very much smaller number of passages than simple circular passages.

(*h*) The cooling-air pressure drop is conveniently rendered non-dimensional by expressing it as a ratio of the dynamic head of the main-stream gas flow leaving the blade row. The resulting cooling-air pressure-drop coefficient, for a given cooled blade row, is then a function primarily of cooling-flow ratio and temperature ratio (T_g/T_{cr}), and to a lesser extent a function of the gas-flow Mach number, and gas-flow Reynolds number. This method of rendering the pressure drop non-dimensional may form a convenient basis for relating rig tests to engine conditions.

NOTATION

(*Note.* Bars over the letter symbols denote mean values along blade span.)

A_c	Total cross-sectional area of cooling passages in one blade
A_m	Total cross-sectional area of metal in one blade in any spanwise position
B	A constant defined by $k_{pc}w_c/\bar{h}_g S_g$
c	Blade chord
D_e	Hydraulic diameter of cooling passage (4 × area/periphery)
e	Exponential constant (2·718)
$f, \bar{f}$	Passage friction coefficient (skin friction per unit area/$\frac{1}{2}\rho_c V_c^2$)
$h_c, \bar{h}_c$	Blade to cooling air heat-transfer coefficient (heat flow per unit time per unit surface area per unit temperature difference)
$h_g, \bar{h}_g$	Gas to blade heat-transfer coefficient
k	Constant defined by $Nu_g^*/(2 \times 10^5)^x$
$k_{pc}, \bar{k}_{pc}$	Specific heat of cooling air at constant pressure, at bulk cooling air temperature T_c
$\bar{K}$	A function defined by equations (12*a*) and (27) in Appendix I
l	Distance along blade span measured from root
L	Total heated span of blade
L^*	Total length of cooling passages (when greater than L)
M_c	Mach number of cooling-air flow
n	Number of cooling passages in one blade
$\bar{N}u_c$	Mean cooling-flow Nusselt number ($\bar{h}_c D_e/\bar{\lambda}_c$)
$Nu_g, \bar{N}u_g$	Gas-flow Nusselt number ($\bar{h}_g c/\lambda_g$)
$\bar{N}u_g^*$	Mean gas-flow Nusselt number when $Re_g = 2 \times 10^5$ and $T_g/\bar{T}_b \rightarrow 1 \cdot 0$
P_c	Total head pressure of cooling air
p_c	Static pressure of cooling air
Pr_c, Pr_g	Prandtl number of cooling air or gas respectively
$r, \bar{r}$	Radius of rotation of blade at any spanwise position, or at mid-span (average)
R	Gas constant
$\bar{R}e_c$	Reynolds number of cooling air in blade passage (defined by hydraulic diameter and gas properties at mean bulk cooling-air temperature)
Re_g	Reynolds number of gas flow over turbine blade (defined by blade chord, outlet relative gas velocity and gas properties at gas temperature T_g)
s	Blade pitch
S_c	Total 'wetted' periphery of cooling passages in one blade at any spanwise position

(68094) B

S_g	Total external periphery of blade profile (*i.e.*, periphery 'wetted' by hot gas stream)
T_b, $\bar{T}_b$	Blade metal temperature (chordwise mean value)
t_c, $\bar{t}_c$	Static bulk temperature of cooling air
T_c, $\bar{T}_c$	Total temperature of cooling air
T_{cr}	Inlet cooling-air temperature (*i.e.*, value of T_c at blade root)
T_g	'Effective' gas temperature (*i.e.*, mean static gas temperature plus $0 \cdot 85 \times$ mean kinetic gas temperature, mean values being taken around the blade profile)
$\bar{U}$	Mean blade peripheral velocity
V_c, $\bar{V}_c$	Cooling-air velocity
V_g	Relative outlet gas velocity from blade row
w_c	Cooling air mass flow/blade
W_g	Gas mass flow/blade
x	An exponent of gas-flow Reynolds number defining the variation of Nusselt number with Reynolds number (*see* equation 1 in Section 3 and equation 20 in Appendix I)
$\bar{X}$	Mean conductance ratio ($\bar{h}_c S_c/\bar{h}_g S_g$) when cooling flow is turbulent
$\bar{X}_l$	Mean conductance ratio when cooling flow is laminar
y	Constant (*see* equation 1 in section 3 and equation 20 in Appendix I)
Z	Passage-shape parameter defined by $(S_c/c)^{1 \cdot 2}/(A_c/c^2)$; a useful figure of merit for cooling-passage configurations when cooling flow is turbulent
Z_l	Passage-shape parameter defined by $(S_c/c)^{1 \cdot 333}/(A_c/c^2)^{0 \cdot 666}$; a useful figure of merit for cooling-passage configurations when cooling flow is laminar
α_2, $\bar{\alpha}_2$	Gas outlet angle from blade row } measured from axial direction
β_1, $\bar{\beta}_1$	Blade inlet angle } measured from axial direction
γ	Ratio of specific heats
λ_c, $\bar{\lambda}_c$	Thermal conductivity of cooling air at bulk cooling air temperature T_c
λ_g	Thermal conductivity of hot gas at gas temperature T_g
λ_m	Thermal conductivity of blade material
μ_c, $\bar{\mu}_c$	Viscosity of cooling air at bulk cooling air temperature T_c
μ_g	Viscosity of hot gas at gas temperature T_g
ρ_c, $\bar{\rho}_c$	Density of cooling air
ρ_g	Density of gas flow at blade outlet
ϕ	Cooling flow ratio (w_c/W_g)
ψ	Cooling-passage shape factor defined by (periphery of a cooling passage)/πD_e
ω	Angular velocity of rotor row

REFERENCES

No.	Author	Title, etc.
1	D. G. Ainley	An experimental single-stage air-cooled turbine. Part II.—Research on the performance of a type of internally air-cooled turbine blade. *Proc. Inst. Mech. Eng.* Vol. 167. 1953.
2	T. W. F. Brown	Effect of the radiation correction on cooling loss in high temperature cooled gas turbines. *Proc. Inst. Mech. Eng.* General discussion on heat transfer. 1951.
3	E. R. G. Eckert	*Introduction to the transfer of heat and mass.* McGraw-Hill. 1950.
4	W. H. McAdams	*Heat transmission.* McGraw-Hill (2nd Edition). 1942.
5	H. B. Squire	Heat-transfer calculations for aerofoils. R. & M. 1986. November, 1942.
6	D. G. Wilson and J. A. Pope ..	Convective-heat transfer to gas-turbine blade surfaces. *Proc. Inst. Mech. Eng.* (1954).
7	S. J. Andrews and P. C. Bradley ..	Heat transfer to turbine blades. N.G.T.E. Memo. No. M37. A.R.C. 12,078. October, 1948.
8	J. E. Hubbart	Comparison of outside-surface heat-transfer coefficients for cascades of turbine blades. N.A.C.A. RM E50C28. (NACA/TIB/2421). (1950).
9	K. Bammert and H. A. Hahnemann	Heat transfer in gas surrounding cooled gas-turbine blades. Part III. R.T.P. No. 620, GDC2466 (MOS). 1946.
10	E. Pohlenan	Temperatures and stresses on hollow blades for gas turbines. N.A.C.A. TM.1183. 1947.
11	L. V. Humble, W. H. Lowdermilk and L. G. Desmon	Measurements of average heat-transfer and friction coefficients for subsonic flow of air in smooth tubes at high surface and fluid temperatures. N.A.C.A. Report 1020. 1951.
12	W. H. Lowdermilk, W. F. Weiland and J. N. B. Livingood	Measurement of heat-transfer and friction coefficients for flow of air in non-circular ducts at high surface temperatures. N.A.C.A. RM E5 3J07(NACA/TIB/3891). 1954.
13	M. Cox and P. S. Lamb	Performance tests on an equal-pressure flame-trap regenerator unit. N.G.T.E. Report No. R.80. November, 1950. ARC 13,919.
14	A. H. Shapiro and W. R. Hawthorne	The mechanics and thermodynamics of steady one-dimensional gas flow. *J. of App. Mech.*, Vol. 14. December, 1947.
15	J. E. Hubbart, H. O. Stone and V. L. Arne	Method for rapid determination of pressure change for one-dimensional flow with heat transfer, friction, rotation and area change. N.A.C.A. Tech. Note 3150. 1954.
16	A. G. Smith and R. D. Pearson ..	The cooled gas turbine. *Proc. Inst. Mech. Eng.*, Vol. 163. 1950.
17	A. G. Smith	Heat flow in the gas turbine. *Proc. Inst. Mech. Eng.*, Vol. 159. 1948.

APPENDIX I

Derivation of Equations Employed for Calculating the Degree of Cooling in a Simple Internally Air-cooled Turbine Blade

Throughout the following analysis it is assumed that the blade is cooled by passing cold air spanwise from root to tip through smooth internal passages which have uniform cross-sectional size and shape throughout their length. The method adopted is in essence a development of that described in Ref. 17.

Selecting an elemental length δl of the blade at a distance l from the root (*see* Fig. 15) the basic differential equation of heat flow is obtained by equating the total rate of heat flow into an element to zero. Thus:

$$\lambda_m A_m \frac{d^2 T_b}{dl^2} + h_g S_g (T_g - T_b) + h_c S_c (T_c - T_b) = 0 . \qquad (1)$$

For the internal air flow through the elemental length, δl, the heat-balance equation is:

$$k_{pc} w_c \frac{dT_c}{dl} + h_c S_c (T_c - T_b) = 0 . \qquad (2)$$

The solution of these equations is greatly simplified if it is assumed that the effect of conduction of heat spanwise along the blade is negligible. This condition is sufficiently fulfilled by turbine blades having conventional values of aspect ratio (2 or more), when constructed of heat-resistant materials. The assumption is only likely to lead to gross error when the aspect ratio is small, or, to a lesser extent, when the operating gas-flow Reynolds number is very small.

Thus, if

$$h_c S_c / h_g S_g = X , \qquad k_{pc} w_c / h_g S_g = B$$

$\lambda_m = 0$ (equivalent to saying that spanwise conduction is negligible), $T_b' = T_g - T_b$, $T_c' = T_g - T_c$, and $dT_g/dl = d^2T_g/dl^2 = 0$ (*i.e.*, uniform gas-temperature distribution), then equations (1) and (2) can be rewritten as:

$$T_b'(1 + X) - XT_c' = 0 \qquad (1a)$$

and

$$\frac{B}{L} \frac{dT_c'}{d(l/L)} - XT_b' + XT_c' = 0 . \qquad (2a)$$

For a cooled turbine blade operating in gas flow of uniform temperature the variation in h_g and k_{pc} along the blade span is relatively small and, providing mean mid-span values of k_{pc} and h_g are employed, it may be assumed that B is a constant. On the other hand the value of h_c may increase appreciably from root to tip, particularly in blades in which a high degree of cooling is obtained with a small quantity of cooling air. In solving equations (1*a*) and (2*a*) therefore, it is desirable to assume that X is some function of l/L.

Solving equations (1*a*) and (2*a*) for T_b' and T_c' yields:

$$T_b' = T_{br}' e^{-K_1} \qquad (3)$$

$$T_c' = T_{cr}' e^{-K_2} \qquad (4)$$

where

$$K_1 = \int_0^{l/L} \left\{ \frac{L}{B} \frac{X}{(1 + X)} - \frac{dX/d(l/L)}{X(1 + X)} \right\} d(l/L) \qquad (5)$$

and

$$K_2 = \int_0^{l/L} \frac{L}{B} \frac{X}{1 + X} d(l/L) . \qquad (6)$$

T_{br}' = value of T_b' at the blade root $= T_g - T_{br}$

T_{cr}' = value of T_c' at the blade root $= T_g - T_{cr}$.

Equation (1*a*) gives:

$$T_{br}' = \frac{X_r}{1 + X_r} T_{cr}' \quad \ldots \quad (7)$$

where X_r = value of X at the blade root.

Thus, combining equations (7) and (3), we have :

$$\frac{T_b - T_{cr}}{T_g - T_{cr}} = 1 - \frac{X_r}{1 + X_r} e^{-K_1}, \quad \ldots \quad (8)$$

and equation (4) may be rewritten as:

$$\frac{T_c - T_{cr}}{T_g - T_{cr}} = 1 - e^{-K_2}. \quad \ldots \quad (9)$$

In an internally air-cooled blade having passages of uniform section along the blade span it is found that the value of X increases roughly linearly from root to tip. It is thus permissible to assume for purposes of calculation that:

$$X = X_r + Y(l/L) \quad \ldots \quad (10)$$

where Y is a constant whose value is dependent upon the blade configuration and operating conditions.

If equation (10) is substituted into equations (5) and (6) the latter may be integrated to give:

$$K_2 = \frac{L}{B}\left\{\left(\frac{l}{L}\right) - \frac{1}{Y}\log_e\left[1 + \frac{Y\left(\frac{l}{L}\right)}{1 + X_r}\right]\right\} \quad \ldots \quad (11)$$

$$K_1 = K_2 - \log_e\left[\frac{1 + \frac{Y}{X_r}\left(\frac{l}{L}\right)}{1 + \frac{Y}{(1 + X_r)}\left(\frac{l}{L}\right)}\right]. \quad \ldots \quad (12)$$

Finally, if the variation in X along the blade span is ignored and X is assumed to remain constant and equal to the mid-span value $\bar{X}$ then the equations for K_1 and K_2 reduce to:

$$K_1 = K_2 = \bar{K} = \frac{L}{B}\left(\frac{\bar{X}}{1 + \bar{X}}\right)\left(\frac{l}{L}\right). \quad \ldots \quad (12a)$$

The expressions (8) and (9) for relative blade and cooling air temperatures then become:

$$\frac{T_b - T_{cr}}{T_g - T_{cr}} = 1 - \frac{\bar{X}}{1 + \bar{X}} e^{-\bar{K}} \quad \ldots \quad (12b)$$

$$\frac{T_c - T_{cr}}{T_g - T_{cr}} = 1 - e^{-\bar{K}}. \quad \ldots \quad (12c)$$

Now in an internally air-cooled rotor blade operating in a stage in which the spanwise distribution of gas temperature is substantially uniform the critical stress/temperature relationship usually occurs in the vicinity of $l/L = 0 \cdot 3$–$0 \cdot 5$. It is particularly important, therefore, that any simple method for calculating the blade temperatures should give a good approximation to the true values in the mid-span region of the blade. It is found that use of the simplest equations (12*a*), (12*b*) and (12*c*) fulfils this condition satisfactorily providing the values selected for $\bar{B}$ and $\bar{X}$ are those equal to the mid-span values in the actual blade. The degree of error involved in making this assumption is illustrated in Fig. 15. These figures relate to the blade operating in the N.G.T.E. Experimental Cooled Turbine No. 117 (Ref. 1), in which the degree of cooling achieved for a given quantity of cooling air was high and in which, as a consequence, the variation in X along the blade span was relatively large. In this instance the variation of X was assumed to be:

$$X = 0{\cdot}72 + 0{\cdot}74\,(l/L) \text{ when } w_c/W_g = 0{\cdot}01$$

and

$$X = 1{\cdot}32 + 0{\cdot}72\,(l/L) \text{ when } w_c/W_g = 0{\cdot}02\,.$$

It will be observed that the maximum error occurs close to the blade root and at low values of cooling-flow ratio, the simple assumption that X = constant = $\bar{X}$ under-estimating the blade-root temperature. On the other hand, from $l/L = 0{\cdot}2$ to $1{\cdot}0$ the simple approximations agree well with the more accurate calculations.

It remains, therefore, to derive suitable values for L/B, $\bar{X}$, and $\bar{K}$ for any blade configuration. The derivation of convenient expressions for these factors is outlined in the following paragraphs.

Note. In the above expressions for relative blade and cooling-air temperatures the value of T_g should, of course, be the 'effective' gas temperature measured relative to the blade. The 'effective' gas temperature may be approximately defined as:

$$T_g = T_{g\,\text{total}}\left[1 - 0{\cdot}15\left\{\frac{\frac{\gamma - 1}{2}\bar{M}^2}{1 + \frac{\gamma - 1}{2}\bar{M}^2}\right\}\right],$$

where $\bar{M}$ is the mean Mach number of the flow around the blade profile.

(*a*) *Internal heat transfer* (*turbulent flow*).—The average rate at which heat passes from blade to cooling per unit temperature difference between blade T_b and cooling air T_c is h_cS_c, which may be expressed as:

$$\bar{h}_cS_c = \frac{\bar{N}u_c\bar{\lambda}_c}{D_e}S_c \qquad \ldots \qquad (13)$$

where $\bar{N}u_c$ = mean cooling-air Nusselt number defined at bulk air temperature

$\bar{\lambda}_c$ = conductivity of cooling air (at mean bulk temperature)

D_e = mean hydraulic diameter of cooling passages

$= 4A_c/S_c$

A_c = total cross-sectional area of all cooling passages in one blade

S_c = total perimeter of all cooling passages in one blade.

From Ref. 11 the following expression for $\bar{N}u_c$ in passages of uniform cross-section may be derived:

$$\bar{N}u_c = 0{\cdot}034P_r^{0{\cdot}4}(L/D_e)^{-0{\cdot}1}(\bar{R}e_c)^{0{\cdot}8}\left(\frac{\bar{T}_c}{\bar{T}_b}\right)^{0{\cdot}55},$$

where conductivity, density and viscosity are all defined at bulk cooling-air temperature. For air in which Pr = Prandtl number = $0{\cdot}71$ and passages of $L/D_e = 25$ to 100 this may adequately be simplified to:

$$\bar{N}u_c = 0{\cdot}02(\bar{R}e_c)^{0{\cdot}8}\left(\frac{\bar{T}_c}{\bar{T}_b}\right)^{0{\cdot}55} \qquad \ldots \qquad (14)^*$$

Now,

$$\bar{R}e_c = \frac{\bar{\rho}_c\bar{V}_cD_e}{\bar{\mu}_c} = \frac{\bar{\rho}_c\bar{V}_cA_c}{\bar{\mu}_c}\frac{D_e}{A_c} = \frac{w_c}{\bar{\mu}_c}\frac{D_e}{A_c}. \qquad \ldots \qquad (15)^*$$

* In applications of equations (14) and (15) the values of $\bar{\mu}_c$ and $\bar{\lambda}_c$ should strictly be evaluated at the bulk mean static temperature of the cooling flow. In practice, however, the mean Mach number of the cooling flow rarely exceeds a value of about $0{\cdot}3$ and a negligible error is introduced by evaluating $\bar{\mu}_c$ and $\bar{\lambda}_c$ at the mean bulk total temperature.

It is desirable to relate $\bar{R}e_c$ to the external gas flow Reynolds number Re_g. Re_g is defined as $(\rho_g V_g c)/\mu_g$ where ρ_g and V_g are values of density and velocity of the main gas stream measured downstream of and relative to the blade row, and μ_g is viscosity evaluated at the temperature T_g.

Thus,

$$Re_g = \frac{\rho_g V_g sLc \cos\alpha_2}{sL\mu_g \cos\alpha_2}$$

$$= \frac{W_g}{\mu_g} \frac{c}{sL \cos\alpha_2}, \quad \ldots \quad (16)$$

where s = blade pitch

α_2 = gas outlet angle

W_g = gas mass flow through one passage.

Therefore, combining (15) and (16) we have:

$$\frac{\bar{R}e_c}{Re_g} = \left(\frac{w_c}{W_g}\right)\left(\frac{LD_e}{A_c}\right)\left(\frac{s}{c}\right)\cos\alpha_2\left(\frac{\mu_g}{\mu_c}\right). \quad \ldots \quad (17)$$

In the air and gas temperature range encountered in gas turbines $\mu \simeq$ constant $\times\ T^{0\cdot62}$, so that $\mu_g/\mu_c = (T_g/T_c)^{0\cdot62}$. Substituting this in equation (17), replacing D_e by $4A_c/S_c$, and denoting the cooling-flow ratio, w_c/W_g, by the symbol ϕ gives:

$$\bar{R}e_c = 4\phi \frac{s}{c}\frac{(L/c)}{(S_c/c)} \cos\alpha_2 \left(\frac{T_g}{\bar{T}_c}\right)^{0\cdot62} Re_g. \quad \ldots \quad (18)$$

Finally, therefore, inserting (18) and (14) into (13) we have

$$\bar{h}_c S_c = 0\cdot02 \left[4\phi \frac{s}{c}\frac{(L/c)}{(S_c/c)} \cos\alpha_2\right]^{0\cdot8} Re_g^{0\cdot8} \left(\frac{\bar{T}_c}{\bar{T}_b}\right)^{0\cdot55} \left(\frac{T_g}{\bar{T}_c}\right)^{0\cdot496} \frac{\bar{\lambda}_c S_c^2}{4A_c}. \quad \ldots \quad (19)$$

(*b*) *External heat transfer*.—It is supposed that the mean external heat-transfer coefficient (*i.e.*, between hot gas and the blade outer surface) is governed by a relationship of the form:

$$\bar{N}u_g = k(Re_g)^x \left(\frac{T_g}{\bar{T}_b}\right)^y. \quad \ldots \quad (20)$$

The constants k, x and y will depend primarily upon the blade shape, and the choice of suitable values is discussed briefly in section 3.

In this relationship $\bar{N}u_g$ is defined as:

$$\bar{N}u_g = \frac{\bar{h}_g c}{\lambda_g} \text{ and } k = Nu_g^*/(2 \times 10^5)^x, \quad \ldots \quad (21)$$

where λ_g is defined at gas temperature T_g.). Re_g has already been defined in the previous paragraph (*see* equation (16)).

Thus equations (20) and (21) lead to the expression:

$$\bar{h}_g S_g = \frac{\bar{N}u_g \lambda_g}{c} S_g$$

$$= k \frac{S_g}{c} \lambda_g \left(Re_g\right)^x \left(\frac{T_g}{\bar{T}_b}\right)^y. \quad \ldots \quad (22)$$

(*c*) *Derivation of expression for* $\bar{X}$ (*turbulent-cooling flow*).—Combining equations (22) and (19) we can arrive at the following expression for $\bar{X}$:

$$\bar{X} = \frac{\bar{h}_c S_c}{\bar{h}_g S_g}$$

$$= \frac{0 \cdot 0152}{k} \frac{\left[\frac{s}{c}\frac{L}{c}\cos\alpha_2\right]^{0 \cdot 8}}{\frac{S_g}{c}} \frac{\left(\frac{S_c}{c}\right)^{1 \cdot 2}}{\frac{A_c}{c^2}} (\phi)^{0 \cdot 8}\left(\frac{\bar{\lambda}_c}{\lambda_g}\right)\left(Re_g\right)^{0 \cdot 8 - x}\left(\frac{\bar{T}_c}{\bar{T}_b}\right)^{0 \cdot 55}\left(\frac{T_g}{\bar{T}_c}\right)^{0 \cdot 496}\left(\frac{\bar{T}_b}{T_g}\right)^{y}. \quad (23)$$

Over the temperature range relevant to gas-turbine engines the conductivity of air may be assumed to vary approximately in proportion to $T^{0 \cdot 77}$, so that the term $(\bar{\lambda}_c/\lambda_g)$ may be replaced by $(\bar{T}_c/T_g)^{0 \cdot 77}$. Furthermore, the ratio of the blade outer periphery to blade chord for a wide variety of typical turbine-blade profiles may be approximately taken as 2·3. Equation (23) then reduces to:

$$\bar{X} = \left\{\frac{0 \cdot 0066}{k}\left(\frac{\bar{s}}{c}\frac{L}{c}\cos\bar{\alpha}_2\right)^{0 \cdot 8} Z\right\} \phi^{0 \cdot 8}(Re_g)^{0 \cdot 8 - x}\left(\frac{\bar{T}_c}{T_g}\right)^{0 \cdot 824}\left(\frac{T_g}{\bar{T}_b}\right)^{0 \cdot 55 - y}, \quad \ldots \quad \ldots \quad (24)$$

where

$$Z = (S_c/c)^{1 \cdot 2}/(A_c/c^2) .$$

In this equation the mean values $\bar{\alpha}_2$, $\bar{s}$, $\bar{T}_c$ and $\bar{T}_b$ are taken to be the values occurring at the mid-span position along the blade. It is worth noting that the expression inside the curly brackets is defined completely by the blade and cooling-passage geometry, and the constant k, which is empirically related with the blade geometry (Fig. 3).

(*d*) *Derivation of expression for* $\bar{K}$.—From equation (12*a*) :

$$\bar{K} = \frac{L}{B}\frac{\bar{X}}{1 + \bar{X}}\left(\frac{l}{L}\right)$$

where $\quad L/B = L\bar{h}_g S_g/\bar{k}_{pc} w_c = L\bar{h}_g S_g/\bar{k}_{pc}\phi W_g .$

Substituting for $\bar{h}_g S_g$ from equation (22) and for W_g from equation (16) we have that:

$$\frac{L}{B} = \frac{k(S_g/c)(T_g/\bar{T}_b)^y}{\phi(Re_g)^{1-x}(\bar{s}/c)\cos\bar{\alpha}_2}\frac{\lambda_g}{\mu_g \bar{k}_{pc}} . \quad \ldots \quad \ldots \quad \ldots \quad \ldots \quad \ldots \quad \ldots \quad (25)$$

Now for air $k_p \propto T^{0 \cdot 15}$, so that:

$$\bar{k}_{pc} = k_{pg}\left(\frac{\bar{T}_c}{T_g}\right)^{0 \cdot 15} .$$

Furthermore, $\mu_g k_{pg}/\lambda_g$ = Prandtl number = $Pr = 0 \cdot 71$ (for air). Equation (25) then becomes:

$$\frac{L}{B} = \frac{k(S_g/c)(T_g/\bar{T}_b)^y (T_g/\bar{T}_c)^{0 \cdot 15}}{Pr\phi(Re_g)^{1-x}(\bar{s}/c)\cos\bar{\alpha}_2} . \quad \ldots \quad \ldots \quad \ldots \quad \ldots \quad \ldots \quad \ldots \quad (26)$$

Finally, therefore, if $S_g/c = 2 \cdot 3$:

$$\bar{K} = \left\{\frac{3 \cdot 24k}{(\bar{s}/c)\cos\bar{\alpha}_2}\right\}\left(\frac{T_g}{\bar{T}_b}\right)^y\left(\frac{T_g}{\bar{T}_c}\right)^{0 \cdot 15}\frac{(l/L)\bar{X}}{\phi(Re_g)^{1-x}(1 + \bar{X})} . \quad \ldots \quad \ldots \quad \ldots \quad (27)$$

Again, it is to be noted that the expression within the curly brackets is defined completely by the blade geometry.

(*e*) *Application of derived formulae to the calculation of the mid-span blade and cooling-air temperatures of a cooled blade (turbulent-cooling flow).*—Summarising previous paragraphs, we have at mid-span ($l/L = 0\cdot5$) that:

$$\frac{\bar{T}_b - T_{cr}}{T_g - T_{cr}} = 1 - \frac{\bar{X}}{1 + \bar{X}} e^{-\bar{K}} \quad \text{(28)}$$

$$\frac{\bar{T}_c - T_{cr}}{T_g - T_{cr}} = 1 - e^{-\bar{K}}, \quad \text{(29)}$$

where

$$\bar{X} = \frac{0\cdot0066}{k}\left(\frac{s}{c}\frac{L}{c}\cos\bar{\alpha}_2\right)^{0\cdot8}\phi^{0\cdot8}Z Re_g^{\,0\cdot8-x}\left(\frac{\bar{T}_c}{T_g}\right)^{0\cdot824}\left(\frac{T_g}{\bar{T}_b}\right)^{0\cdot55-y} \quad \text{(30)}$$

$$\bar{K} = \left\{\frac{3\cdot24k}{s/c\cos\bar{\alpha}_2}\right\}\frac{l/L}{\phi Re_g^{\,1-x}}\frac{\bar{X}}{1+\bar{X}}\left(\frac{T_g}{\bar{T}_b}\right)^{y}\left(\frac{T_g}{\bar{T}_c}\right)^{0\cdot15}, \quad \text{(31)}$$

and

$$l/L = 0\cdot5$$

L, s, c, $\bar{\alpha}_2$, k, x, y and z are fixed by the blade and cooling-passage geometry and by the assumed relationship between $\bar{N}u_g$ and Re_g (*see* section (*b*)). Selecting desired values for ϕ, Re_g, T_g and T_{cr} we then have at mid-span that:

$$\bar{X} = \text{constant}\left\{\left(\frac{\bar{T}_c}{T_g}\right)^{0\cdot824}\left(\frac{T_g}{\bar{T}_b}\right)^{0\cdot55-y}\right\},$$

$$K = \text{constant}\frac{\bar{X}}{(1+\bar{X})}\left\{\left(\frac{T_g}{\bar{T}_b}\right)^{y}\left(\frac{T_g}{\bar{T}_c}\right)^{0\cdot15}\right\}.$$

It is now necessary to make a preliminary guess at the values of $\bar{T}_b$ and $\bar{T}_c$ and to find the corresponding values of $\bar{X}$ and $\bar{K}$. These are then substituted in equations (28) and (29), from which a first good approximation to the actual values of $\bar{T}_b$ and $\bar{T}_c$ may be derived. If the values of $\bar{X}$ and $\bar{K}$ are then recalculated using the latter values of $\bar{T}_b$ and $\bar{T}_c$ and resubstituted into equations (28) and (29) a second closer approximation to the actual values of $\bar{T}_b$ and $\bar{T}_c$ may be found. This may be continued to further, and closer, approximations but the approximations will be found to be very rapidly convergent to the correct values and it will very seldom be necessary to proceed beyond the second approximations.

The values of T_b and T_c at spanwise positions other then at $l/L = 0\cdot5$ may be calculated by a similar procedure. The appropriate value of l/L must be inserted into equation (31) and the values $\bar{T}_c$ and $\bar{T}_b$ in equations (28) to (31) must be replaced by the values of T_c and T_b appropriate to the spanwise position considered.

(*f*) *Approximate method of allowing for the heat picked up by the cooling air in the blade root (turbulent-cooling flow).*—In many constructional arrangements the blade cooling air will, in addition to cooling the blade itself, also cool the blade root and, in particular, the blade-root platform. Since the cooling of the root and platform will preheat the cooling air before it enters the blade proper then the cooling of the blade itself will be rather less than that which would be calculated by the previous method if the root cooling was ignored. It is desirable, therefore, to devise a simple method of correcting for this effect.

It will be assumed that:

(i) the heat passed into the blade root (equal to the heat collected by the entry cooling air) enters only across the blade-root–platform area exposed to the hot gas stream (suppose this area is A_p)

(ii) the mean heat-transfer coefficient between gas and platform is equal to the mean heat-transfer coefficient between the gas and blade

(iii) the blade-platform temperature is equal to the temperature of the blade-root section.

Assumption (ii) is probably pessimistic since the actual values of gas to platform heat-transfer coefficient will probably be lower, in practice, than the assumed values. This may be partially counter-balanced, however, by the fact that heat may creep into the blade root by conduction, convection and radiation from sources other than the scrubbed area of the platform defined in assumption (i). Since the total effect of root and disc-rim cooling is not very great these assumptions are unlikely to give highly erroneous results and enable a correction to be made quite simply as follows.

Assumptions (i) and (ii) enable the actual root to be visualised as being equivalent, from a point of view of the heat transfer, to an imaginary extension at the root end of the actual blade length by an amount equal to $(A_p/A_b)L$, where A_p = platform area and A_b = actual blade surface area. This imaginary extension of the blade length must be accompanied by an imaginary extension of the gas stream (and gas-flow quantity) of the same proportion.

Now in equations (28) to (31) the value of the conductance ratio $\bar{X}$, will not be influenced by the imaginary extension of the blade. A modification will occur only to the parameter $\bar{K}$ which controls the rate at which the cooling air is heated as it flows through the cooling passages.

Using a dash suffix to indicate values measured relative to the imaginary blade of extended length then equation (31) for $\bar{K}$ may be rewritten as:

$$\bar{K} = \left\{\frac{3 \cdot 24k}{(s/c) \cos \bar{\alpha}_2}\right\} \frac{\left(\frac{l'}{L'}\right)}{\phi'(Re_g)^{1-x}} \frac{\bar{X}}{1 + \bar{X}} \left(\frac{T_g}{\bar{T}_b}\right)^y \left(\frac{T_g}{\bar{T}_c}\right)^{0 \cdot 15}, \quad \ldots \quad (32)$$

and

$$\left.\begin{aligned} l' &= l + \frac{A_p}{A_b} L \\ L' &= L + \frac{A_p}{A_b} L \\ \phi' &= \frac{\phi}{1 + \frac{A_p}{A_b}} \end{aligned}\right\} . \quad \ldots \quad (33)$$

The 'effective' value of ϕ' arises as a result of the imaginary extension of the gas stream, consequent upon the imaginary blade extension, which is not accompanied by any change in the quantity of cooling air through the blade.

Substituting equations (33) into equation (32) yields:

$$\bar{K} = \frac{3 \cdot 24k}{\{(s/c) \cos \bar{\alpha}_2\}} \frac{\bar{X}}{1 + \bar{X}} \frac{\frac{l}{L} + \frac{A_p}{A_b}}{\phi Re_g^{1-x}} \left(\frac{T_g}{\bar{T}_b}\right)^y \left(\frac{T_g}{\bar{T}_c}\right)^{0 \cdot 15} \quad \ldots \quad (34)$$

where, as before, l/L has a value of $0 \cdot 5$.

The procedure for calculating the mean blade and cooling-air temperature ($\bar{T}_b$ and $\bar{T}_c$) is then as described in section (*e*).

As before, the values of T_b and T_c at sections other than $l/L = 0 \cdot 5$ may be calculated by substituting the appropriate value of l/L in equation (34) and replacing $\bar{T}_b$ and $\bar{T}_c$ in equations (28), (29), (30) and (34) by the values of T_b and T_c at the particular spanwise position considered.

(*g*) *Cooling with laminar flow in the cooling passages.*—Using a similar procedure to that outlined in the previous paragraphs a set of equations for mean blade temperatures with laminar-cooling flow may be derived. The major difference lies only in the governing equation for coolant-flow Nusselt number, it being assumed that with laminar flow:

$$\bar{N}u_c = 1 \cdot 66 \left[\frac{\bar{R}e_c}{(L/D_e)}\right]^{0 \cdot 333} \quad \ldots \quad (35)$$

(*see* section 4.2)

The full derivation of the equations for blade temperature is not given here, but, following the procedure of the pɪevious paragraphs, it may easily be shown that for laminar-cooling flow :

$$\frac{T_b - T_{cr}}{T_g - T_{cr}} = 1 - \frac{\bar{X}_l}{1 + \bar{X}_l} \mathrm{e}^{-\bar{K}_l}$$

$$\frac{T_c - T_{cr}}{T_g - T_{cr}} = 1 - \mathrm{e}^{-\bar{K}_l}$$

where

$$\bar{X}_l = \left\{\frac{0 \cdot 456}{k} \left[(\cos \alpha_2) \left(\frac{\bar{s}}{c}\right)\right]^{0 \cdot 333} Z_l\right\} \phi^{0 \cdot 333} Re_g^{\,0 \cdot 333 - x} \left(\frac{\bar{T}_c}{T_g}\right)^{0 \cdot 56} \left(\frac{\bar{T}_b}{T_g}\right)^y \quad .. \quad (36)$$

$$\dot{Z}_l = \left(\frac{S_c}{c}\right)^{1 \cdot 333} \Big/ \left(\frac{A_c}{c^2}\right)^{0 \cdot 666} \quad .. \quad .. \quad .. \quad .. \quad .. \quad .. \quad .. \quad (37)$$

$$\bar{K}_l = \left\{\frac{3 \cdot 24k}{(\bar{s}/c) \cos \bar{\alpha}_2}\right\} \left(\frac{T_g}{\bar{T}_b}\right)^y \left(\frac{T_g}{\bar{T}_c}\right)^{0 \cdot 15} \frac{(l/L)\bar{X}_l}{\phi Re_g^{\,1-x}(1 + \bar{X}_l)} . \quad .. \quad .. \quad .. \quad (38)$$

With laminar-cooling flow it is seen from equations (36) and (37) that the influence of cooling passage shape and size is wholly characterized by the cooling passage shape number Z_l. This number differs from the shape number, Z, appropriate to turbulent-cooling flow and it is of interest to find a relationship between the two.

Now,

$$Z = (S_c/c)^{1 \cdot 2}/(A_c/c^2)$$

$$Z_l = (S_c/c)^{1 \cdot 333}/(A_c/c^2)^{0 \cdot 666}$$

and

$$D_e/c = 4(A_c/c^2)/(S_c/c)$$

from which:

$$Z_l = \frac{Z^{3 \cdot 333}(D_e/c)^{2 \cdot 666}}{40 \cdot 2} . \quad .. \quad .. \quad .. \quad .. \quad .. \quad .. \quad .. \quad (39)$$

APPENDIX II

Derivation of Approximate Formulae for Cooling-Air Pressure Loss

(*a*) *Turbulent flow.*—It is demonstrated in Ref. 14 that for one-dimensional flow in a passage of constant cross-sectional area with friction, heat addition, and a centrifugal acceleration in the direction of flow the change of total head pressure along an incremental length of passage δl is given by:

$$\frac{\delta P_c}{P_c} = -\frac{\gamma M_c^2}{2} \frac{\delta T_c}{T_c} - \frac{\gamma M_c^2}{2} 4f \frac{\delta l}{D_e} + \frac{r\omega^2}{Rt_c} \delta l , \quad .. \quad .. \quad .. \quad .. \quad (1)$$

and

$$M_c = V_c/\sqrt{(\gamma p_c/\rho_c)} , \quad .. \quad .. \quad .. \quad .. \quad .. \quad .. \quad .. \quad (2)$$

where

P_c = total head pressure of cooling air

T_c = total temperature of cooling air

M_c = Mach number of flow of cooling air

γ = ratio of specific heats

f = skin-friction coefficient

D_e = hydraulic diameter of passage

r = radius of rotation of blade at spanwise position l

ω = angular velocity of rotation

R = cooling-air gas constant

t_c = static temperature of cooling air

V_c = cooling-air velocity

ρ_c = cooling-air density

p_c = static pressure of cooling air.

It is desirable to express the overall total pressure loss for the blade passage as a fraction of the dynamic head of the gas flow leaving the blade row, $\frac{1}{2}\rho_g V_g^2$ (*see* section 6). A fairly simple equation may be derived if the simplifying assumption is made that M_c is small so that $p_c \rightarrow P_c$ and $t_c \rightarrow T_c$.

Using equations (1) and (2) it can then be shown that for an incremental length of passage, δl:

$$\frac{\delta P_c}{\frac{1}{2}\rho_g V_g^2} = -\frac{\rho_c V_c^2}{\rho_g V_g^2}\frac{\delta T_c}{T_g} - \frac{\rho_c V_c^2}{\rho_g V_g^2} 4f \frac{\delta l}{D_e} + 2\frac{\rho_c U^2}{\rho_g V_g^2}\frac{\delta l}{r}, \quad \ldots \quad (3)$$

where U = peripheral speed of blade = ωr.

By employing Reynolds analogy it is possible to relate $\delta T_c/T_c$ to friction coefficient f. Reynolds analogy may be written:

$$h_c k_{pc}\rho_c V_c = f/2 .$$

Equating heat flows we have also:

$$S_c h_c (T_b - T_c)\delta l = \rho_c V_c A_c k_{pc} \delta T_c$$

whence

$$\frac{\delta T_c}{T_c} = \left(\frac{T_b}{T_c} - 1\right)\frac{S_c}{A_c}\frac{h_c}{k_{pc}\rho_c V_c}\delta l .$$

Therefore

$$\frac{\delta T_c}{T_c} = \left(\frac{T_b}{T_c} - 1\right) 2f\frac{\delta l}{D_e}. \quad \ldots \quad (4)$$

Inserting equation (4) into equation (3) yields:

$$\frac{\delta P_c}{\frac{1}{2}\rho_g V_g^2} = -2\frac{\rho_c V_c^2}{\rho_g V_g^2}\left(1 + \frac{T_b}{T_c}\right) f\frac{\delta l}{D_e} + 2\left(\frac{\rho_c}{\rho_g}\right)\left(\frac{U}{V_g}\right)^2 \frac{\delta l}{r}$$

$$= -2\frac{\rho_g}{\rho_c}\phi^2\left(\frac{A_t}{A_c}\right)^2\left(1 + \frac{T_b}{T_c}\right) f\frac{\delta l}{D_e} + 2\frac{\rho_c}{\rho_g}\left(\frac{U}{V_g}\right)^2\frac{\delta l}{r}. \quad \ldots \quad (5)$$

Now

$$A_t = Ls \cos \bar{\alpha}_2.$$

Therefore

$$\left(\frac{A_t}{A_c}\right)^2 = \left[\frac{sL \cos \bar{\alpha}_2}{A_c}\right]^2. \quad \ldots \quad (6)$$

If equation (6) is now inserted into equation (5) and if in addition δl is replaced by the full passage length L^* (which may be greater than the length of the heated span of the blade L) and a mean value $(\bar{\rho}_c/\rho_g)$ is approximated by $(T_g/\bar{T}_c)$ then:

$$\frac{P_{c\,\text{inlet}} - P_{c\,\text{outlet}}}{\frac{1}{2}\rho_g V_g^2} = 2f\left(\frac{\bar{T}_c}{T_g}\right)\left(1 + \frac{\bar{T}_b}{\bar{T}_c}\right)\left(\phi\frac{sL}{A_c}\cos\bar{\alpha}_2\right)^2\frac{L^*}{D_e}$$

$$- 2\left(\frac{T_g}{\bar{T}_c}\right)\left(\frac{\bar{U}}{V_g}\right)^2\frac{L^*}{\bar{r}}, \quad \ldots \quad (7)$$

where $\bar{r}$ = mean radius of rotor-blade row.

If the cooling air is discharged from the blade tips in such a way that the full outlet dynamic head of the cooling air $(\frac{1}{2}\rho_c V_c^2)_{\text{exit}}$, is lost then it may be shown that approximately:

$$\frac{(\frac{1}{2}\rho_c V_c^2)_{\text{exit}}}{\frac{1}{2}\rho_g V_g^2} = \left(\phi\frac{sL}{A_c}\cos\bar{\alpha}_2\right)^2\frac{T_{c\,\text{tip}}}{T_g}. \quad \ldots \quad (8)$$

Combining (7) and (8) we have:

$$\frac{P_{c\,\text{inlet}} - p_{c\,\text{outlet}}}{\frac{1}{2}\rho_g V_g^2} = 2\bar{f}\left(\frac{\bar{T}_c}{T_g}\right)\left(1 + \frac{\bar{T}_b}{\bar{T}_c}\right)\left(\phi\frac{sL}{A_c}\cos\bar{\alpha}_2\right)^2\frac{L^*}{D_e}$$

$$+\left(\phi\frac{sL}{A_c}\cos\bar{\alpha}_2\right)^2\left(\frac{T_{c\,\text{tip}}}{T_g}\right) - 2\left(\frac{T_g}{\bar{T}_c}\right)\left(\frac{\bar{U}}{V_g}\right)\frac{L^*}{\bar{r}}. \quad \ldots \quad (9)$$

The mean skin-friction coefficient, $\bar{f}$, for turbulent flow in a passage is given by:

$$\bar{f} = \frac{0\cdot079}{(\bar{R}e_c)^{0\cdot25}}. \quad \ldots \quad (10)$$

A relationship between $\bar{R}e_c$ and Re_g is derived in equation (17) of Appendix I. If this relationship is introduced into equation (10) then:

$$\bar{f} = \frac{0\cdot079\left(\frac{\bar{T}_c}{T_g}\right)^{0\cdot155}}{\left(\phi\frac{sL}{A_c}\cos\bar{\alpha}_2\right)^{0\cdot25}\left(\frac{D_e}{c}\right)^{0\cdot25}\left(Re_g\right)^{0\cdot25}}. \quad \ldots \quad (10a)$$

Introducing equation (10a) into equation (9) then yields:

$$\frac{P_{c\,\text{inlet}} - p_{c\,\text{outlet}}}{\frac{1}{2}\rho_g V_g^2} = \frac{0\cdot158\left(\frac{\bar{T}_c}{T_g}\right)^{1\cdot155}\left(1 + \frac{\bar{T}_b}{\bar{T}_c}\right)\left(\phi\frac{sL}{A_c}\cos\bar{\alpha}_2\right)^{1\cdot75}\frac{L^*}{D_e}}{\left(\frac{D_e}{c}\right)^{0\cdot25}\left(Re_g\right)^{0\cdot25}}$$

$$+\left(\phi\frac{sL}{A_c}\cos\bar{\alpha}_2\right)^2\left(\frac{T_{c\,\text{tip}}}{T_g}\right)$$

$$-2\left(\frac{T_g}{\bar{T}_c}\right)\left(\frac{\bar{U}}{V_g}\right)^2\frac{L^*}{\bar{r}}. \quad \ldots \quad (11)$$

The first term on the right-hand side of equation (11) is the loss due to friction and heat addition, the second term is the cooling-air dynamic head lost at discharge from the blade tip, and the third term (applicable only to rotor blades) is the centrifugal compression due to the rotation of the blade row. In general it is found that with passage configurations giving good cooling ($Z > 150$) the major part of the loss is due to friction and heat addition, the remaining two losses being relatively small and opposite in sign.

A typical break-down of the components of the total overall cooling air pressure drop is given in the table below for the 'datum' blade defined in section 7 when $Z = 200$, $(D_e/c) = 0\cdot025$, $L/c = 2$, $L^*/c = 2\cdot5$, $T_g/T_{cr} = 2\cdot0$, $U/V_g = 0\cdot87$, $L^*/\bar{r} = 0\cdot35$.

Cooling-flow ratio ϕ	0·01	0·02
$\frac{\Delta P}{\frac{1}{2}\rho_g V_g^2}$ due to friction and heat addition	0·53	1·58
$\frac{\Delta P}{\frac{1}{2}\rho_g V_g^2}$ due to discharge loss from blade tip	0·143	0·493
$\frac{\Delta P}{\frac{1}{2}\rho_g V_g^2}$ due to centrifugal compression	−0·614	−0·680
Overall loss $\frac{P_{c\,\text{inlet}} - p_{c\,\text{outlet}}}{\frac{1}{2}\rho_g V_g^2}$	0·039	1·393

It may be noted from equation (11) that blades having different cooling passage configurations but identical external geometry and gas operating conditions will have similar pressure-drop characteristics if the values of A_c and D_e are the same for each configuration. This is equivalent to saying that the pressure-drop characteristics will be similar if the values of Z and (D_e/c) are the same for each cooling passage configuration.

(*b*) *Laminar flow*.—An equation of similar form to equation (11) may be derived for laminar flow in the passages. The major difference arises from the modified relationship between friction coefficient $\bar{f}$, and cooling-flow Reynolds number, $\bar{Re}_c$, for laminar flow. If the temperature ratio $(\bar{T}_b/\bar{T}_c)$ is close to unity then:

$$\bar{f} = \frac{16}{\bar{Re}_c} \qquad \text{(12)}$$

If $(\bar{T}_b/\bar{T}_c)$ is appreciably greater than unity then some unpublished work indicates that a better approximation is:

$$\bar{f} = \frac{16}{\bar{Re}_c}\left(\frac{\bar{T}_b}{\bar{T}_c}\right)^{0 \cdot 45} \qquad \text{(12a)}$$

If the relationship between $\bar{Re}_c$ and Re_g (equation (17) of Appendix I) is introduced into equation (12*a*) then:

$$\bar{f} = \frac{16\left(\frac{\bar{T}_b}{\bar{T}_c}\right)^{0 \cdot 45}\left(\frac{\bar{T}_c}{T_g}\right)^{0 \cdot 62}}{\left(\phi \frac{sL}{A_c} \cos \bar{\alpha}_2\right)\left(\frac{D_e}{c}\right) Re_g} \qquad \text{(12b)}$$

Introducing equation (12*b*) into equation (9) finally yields:

$$\frac{P_{c\,\text{inlet}} - p_{c\,\text{outlet}}}{\frac{1}{2}\rho_g V_g^{\,2}} = \frac{32\left(\frac{\bar{T}_c}{T_g}\right)^{1 \cdot 62}\left(\frac{\bar{T}_b}{\bar{T}_c}\right)^{0 \cdot 45}\left(1 + \frac{\bar{T}_b}{\bar{T}_c}\right)\left(\phi \frac{sL}{A_c} \cos \bar{\alpha}_2\right)\frac{L^*}{D_e}}{\left(\frac{D_e}{c}\right) Re_g}$$

$$+ \left(\phi \frac{sL}{A_c} \cos \bar{\alpha}_2\right)^2\left(\frac{T_{c\,\text{tip}}}{T_g}\right) - 2\left(\frac{T_g}{\bar{T}_c}\right)\left(\frac{\bar{U}}{V_g}\right)^2\frac{L^*}{r} \qquad \text{(13)}$$

As for turbulent flow it will be found that for blades of practical interest with laminar internal flow the major part of the loss is that due to friction and heat transfer (first term on right-hand side of equation (13)). Also different passage configurations will give similar pressure-drop characteristics in a blade of fixed external geometry and operating conditions if A_c and D_e are similar, *i.e.*, if Z, or Z_l, and D_e/c are similar.

(*c*) *Note on influence of* Re_g.—It is of interest to determine the variation of the cooling-flow ratio, ϕ, with gas-flow Reynolds number, Re_g, when all other factors (including pressure-drop coefficient $(P_{c\,\text{inlet}} - p_{c\,\text{outlet}})/(\frac{1}{2}\rho_g V_g^2)$ remain constant. These conditions apply to the particular case of an air-cooled aircraft engine operating at fixed non-dimensional speed over a range of altitude.

Since the major part of the cooling-air pressure drops are contained in the first terms on the right-hand side of equations (11) and (13), for turbulent and laminar flow respectively, then it may be seen that to a first approximation:

$$\phi \propto Re_g^{(0 \cdot 25/1 \cdot 75)} \propto Re_g^{0 \cdot 14} \qquad \text{for turbulent flow}$$

and

$$\phi \propto Re_g \qquad \text{for laminar flow.}$$

If, therefore, the cooling air to the blades is metered solely by the pressure drop occurring across the blade cooling passages (this possibly represents the simplest conceivable arrangement in an engine) then the variation of cooling-flow ratio with Re_g will be relatively small when the cooling flow is turbulent, but large when the flow is laminar. The possible consequences of this are discussed in section 8.

(*d*) *Influence of compressibility* (*turbulent flow*).—Equation (11) is only strictly correct when the Mach numbers of the main gas flow and cooling flow are very small. It is possible however to frame an approximate correction to equation (11) for higher relative outlet Mach numbers of the main gas flow at exit from the blade ($0\cdot1 < M_2 < 0\cdot9$) as follows:

$$\frac{P_{c\,\mathrm{inlet}} - p_{c\,\mathrm{exit}}}{P_{g\,\mathrm{tot}\,2} - p_{g\,\mathrm{stat}\,2}} = \chi \simeq \left\{\overbrace{1 + \chi \frac{\gamma M_2^2}{4}\left(1 + \frac{M_2^2}{4}\right)}^{\text{1st term R.H.S. of equation (11)}}\right\} + \left\{\text{remaining terms in equation (11)}\right\} \qquad (14)$$

The above equation is derived on the assumption that $p_{c\,\mathrm{exit}} \simeq p_{g\,\mathrm{stat}\,2}$. [$P_{g\,\mathrm{tot}\,2}$ = relative outlet total pressure of main gas flow; $p_{g\,\mathrm{stat}\,2}$ = outlet static pressure of main gas flow.]

APPENDIX III

Derivation of 'Effective' Passage-Shape Parameter when Passages in One Blade are of Varying Size and Shape (Turbulent Flow)

If the cooling passages in a blade are not all of equal size and shape then equation (24) of Appendix I, for $\bar{X}$, should be rewritten as:

$$\bar{X} = \frac{0\cdot0066}{k}\left(\cos\bar{\alpha}_2 \frac{s}{c}\frac{L}{c}\right)^{0\cdot8} Re_g^{\,0\cdot8-x}\left(\frac{\bar{T}_c}{T_g}\right)^{0\cdot824}\left(\frac{T_g}{\bar{T}_b}\right)^{0\cdot55-y} \sum_{r=1}^{n}(Z_r\phi_r^{\,0\cdot8}) \quad .. \quad (1)$$

where Z_r and ϕ_r refer to the values of $(S_{cr}/c)^{1\cdot2}/(A_{cr}/c^2)$ and cooling-flow ratio for each individual passage.

Now the pressure-drop coefficients, $\Delta P_c/(\frac{1}{2}\rho_g V_g^2)$, for the cooling air flowing through each of the passages will all be equal. If the major part of the pressure drop is due to skin friction and heat addition (1st term on right-hand side of equation (11), Appendix II) and the pressure-drop coefficients in all passages are equal then equation (11) of Appendix II indicates that, approximately:

$$\phi_r^{\,1\cdot75} \propto A_{cr}^{\,1\cdot75} D_{er}^{\,0\cdot25}$$

i.e.,

$$\phi_r = \text{constant} \times A_{cr} D_{er}^{\,0\cdot143}$$

$$= \text{constant} \times \frac{A_{cr}^{\,1\cdot143}}{S_{cr}^{\,0\cdot143}}, \quad .. \quad .. \quad .. \quad .. \quad .. \quad .. \quad .. \quad (2)$$

whence

$$\phi = \sum_{r=1}^{n}\phi_r = \text{constant}\sum_{r=1}^{n}\frac{A_{cr}^{\,1\cdot143}}{S_{cr}^{\,0\cdot143}}. \quad .. \quad .. \quad .. \quad .. \quad .. \quad (3)$$

Therefore

$$\frac{\phi_r}{\phi} = \frac{\left(\dfrac{A_{cr}^{\,1\cdot143}}{S_{cr}^{\,0\cdot143}}\right)}{\sum_{r=1}^{n}\left(\dfrac{A_{cr}^{\,1\cdot143}}{S_{cr}^{\,0\cdot143}}\right)} \quad .. \quad .. \quad .. \quad .. \quad .. \quad .. \quad .. \quad .. \quad (4)$$

Now the summation term at the end of equation (1) may be rewritten as:

$$\sum_{r=1}^{n} \phi_r^{0\cdot 8} Z_r = \phi^{0\cdot 8} Z_{\text{effective}}\,, \qquad (5)$$

where

$$Z_{\text{effective}} = \sum_{r=1}^{n} \left(\frac{\phi_r}{\phi}\right)^{0\cdot 8} Z_r = c^{0\cdot 8} \sum_{r=1}^{n} \left(\frac{\phi_r}{\phi}\right)^{0\cdot 8} \frac{S_{cr}^{\;1\cdot 2}}{A_{cr}}\,. \qquad (6)$$

Substituting equation (4) into equation (6) yields :

$$Z_{\text{effective}} = \frac{c^{0\cdot 8} \displaystyle\sum_{r=1}^{n} \frac{S_{cr}^{\;1\cdot 086}}{A_{cr}^{\;0\cdot 086}}}{\left\{\displaystyle\sum_{r=1}^{n} \frac{A_{cr}^{\;1\cdot 143}}{S_{cr}^{\;0\cdot 143}}\right\}^{0\cdot 8}}\,. \qquad (7)$$

Finally, substituting equation (5) in equation (1) gives:

$$\bar{X} = \frac{0\cdot 0066}{k}\left(\cos \bar{\alpha}_2 \frac{s}{c}\frac{L}{c}\right)^{0\cdot 8} \phi^{0\cdot 8} Z_{\text{effective}}\, Re_g^{\;0\cdot 8 - x}\left(\frac{\bar{T}_c}{T_g}\right)^{0\cdot 824}\left(\frac{T_g}{\bar{T}_b}\right)^{0\cdot 55 - y}$$

where $Z_{\text{effective}}$ is defined by equation (7).

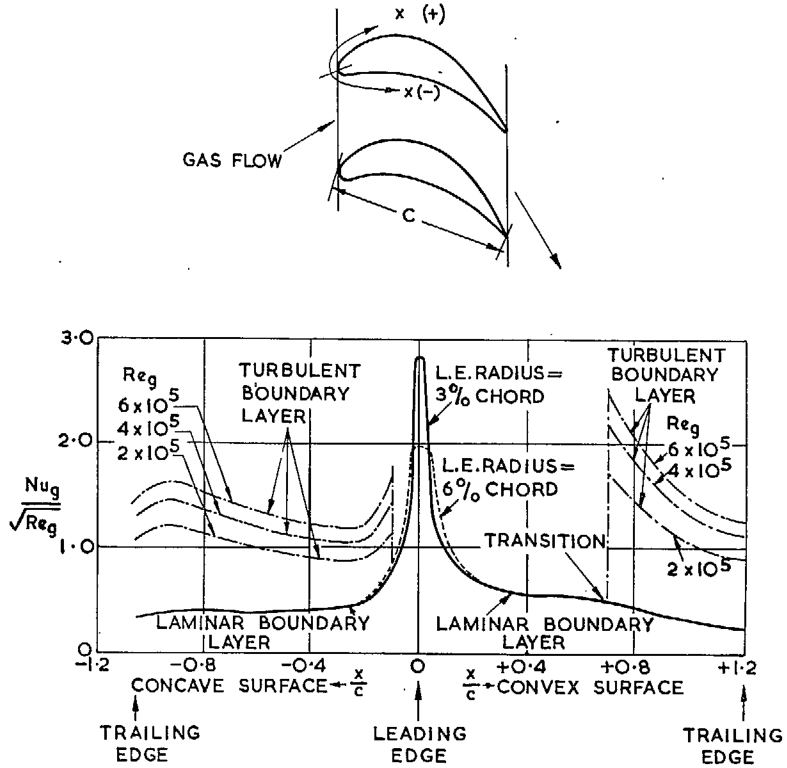

FIG. 1. Variation of heat-transfer coefficient round the surface of a typical turbine blade.

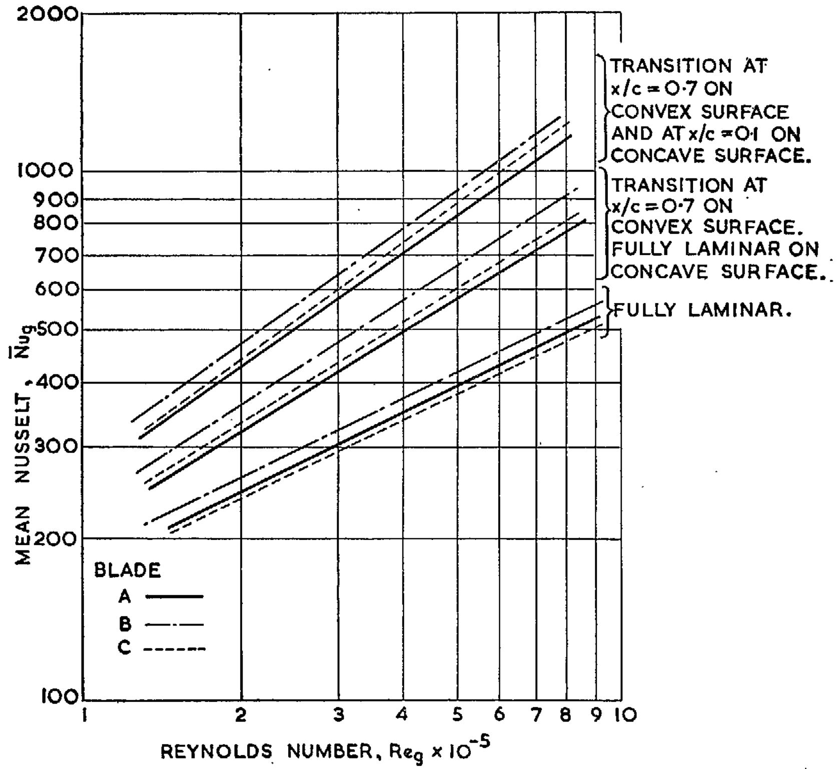

BLADE	A	B	C
α_1	15°	45°	30°
α_2	60°	50°	60°
s/c	0·55	0·62	0·58

FIG. 2. Variation of mean Nusselt number with Reynolds number for various turbine blades (calculated).

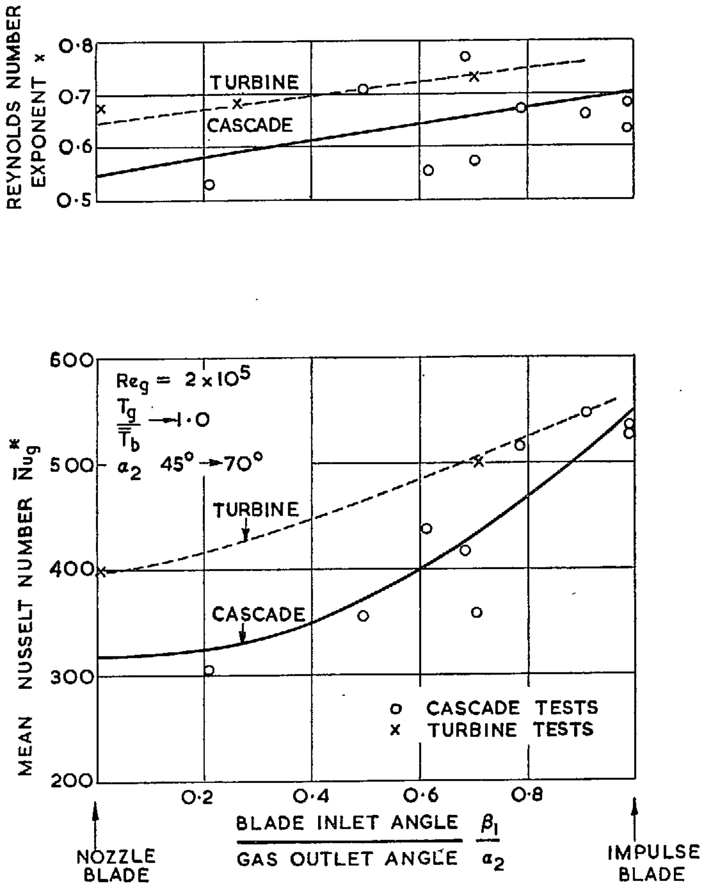

GENERAL EXPRESSION

$$\bar{N}u_g = K \; Re_g^{\,x} \, (T_g/\bar{T}_b)^y$$

$$K = \bar{N}u_g^* / (2 \times 10^5)^x$$

$$y = 0{\cdot}14 \times (Re_g / 2 \times 10^5)^{-0{\cdot}4}$$

FIG. 3. Correlation of external heat-transfer data for a wide range of turbine blades.

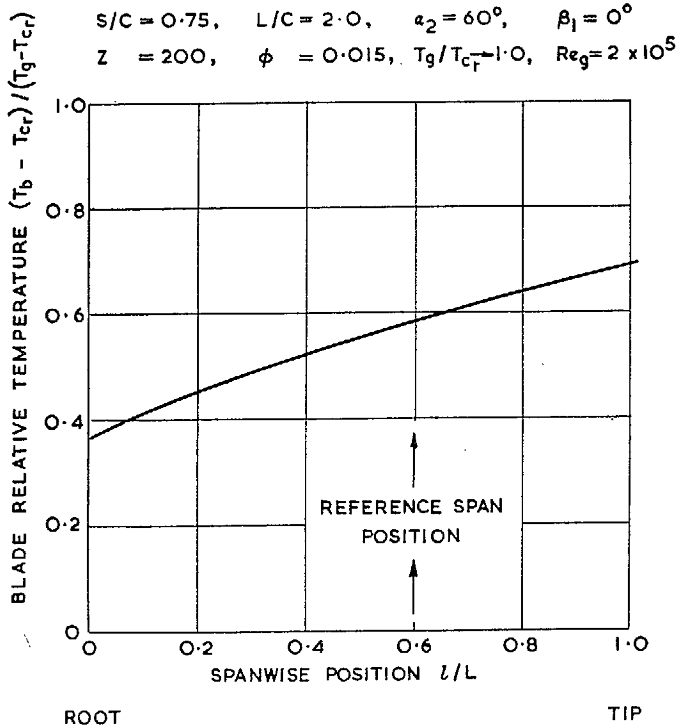

FIG. 4. Spanwise variation of temperature in reference blade.

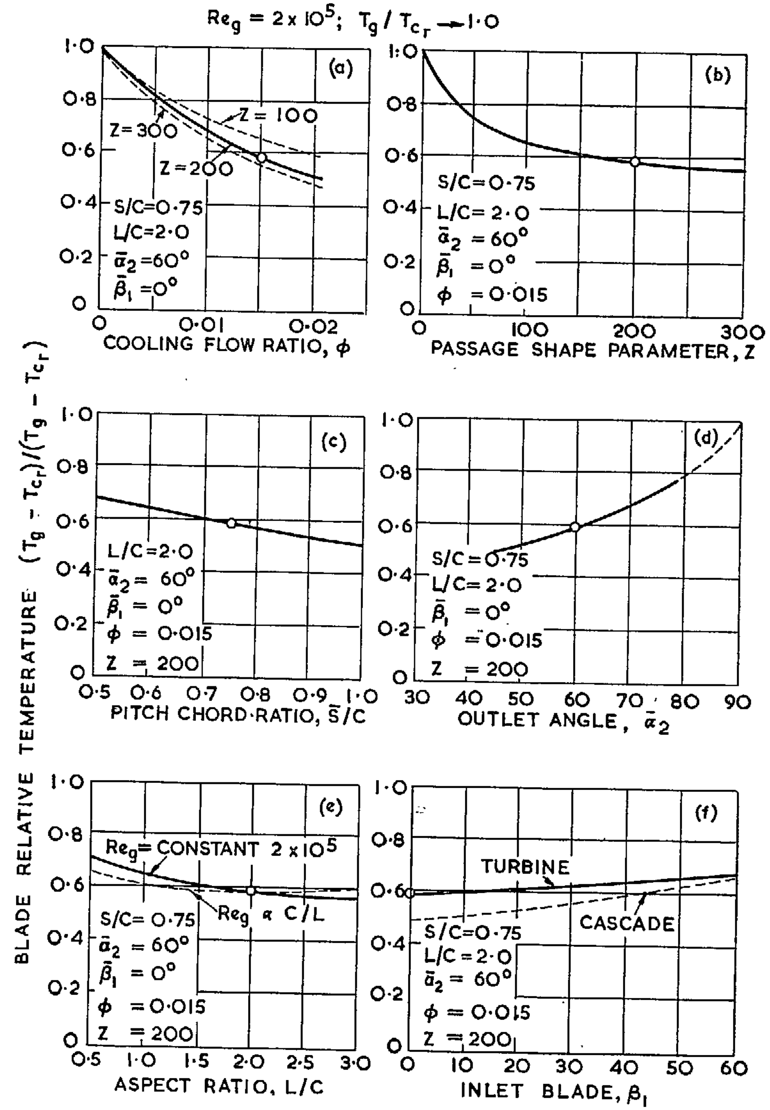

FIGS. 5a to 5f. Influence of various design parameters on blade cooling in reference blade at $l/L = 0 \cdot 6$.

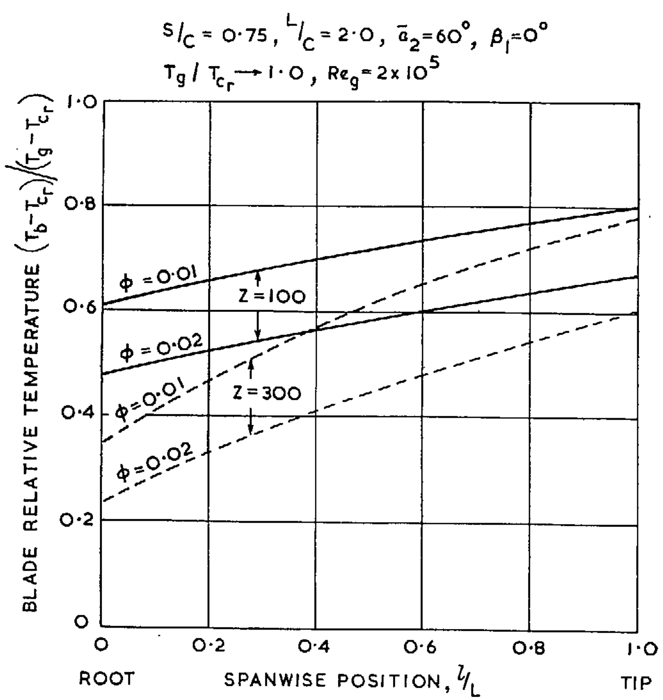

FIG. 6. Influence of passage-shape parameter, Z, and cooling-flow ratio, ϕ, on spanwise temperature distribution reference blade.

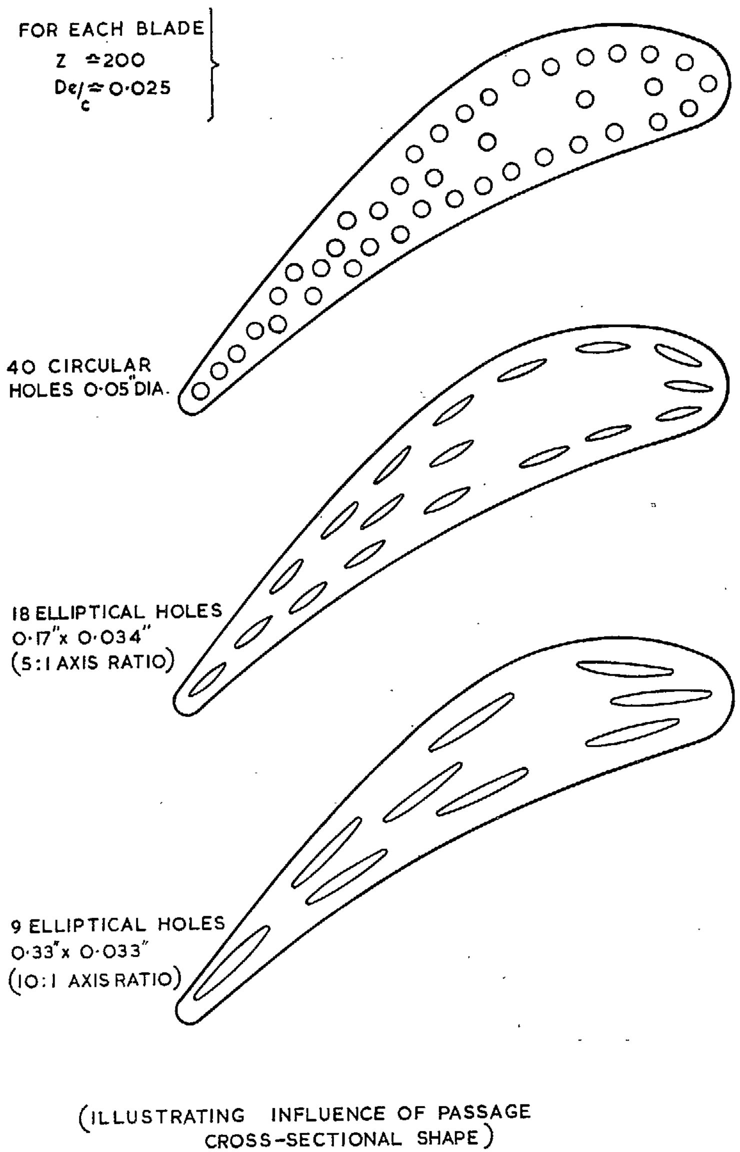

FIG. 7. Three cooling passage configurations giving similar cooling and pressure-loss characteristics. Blade chord 2 in.

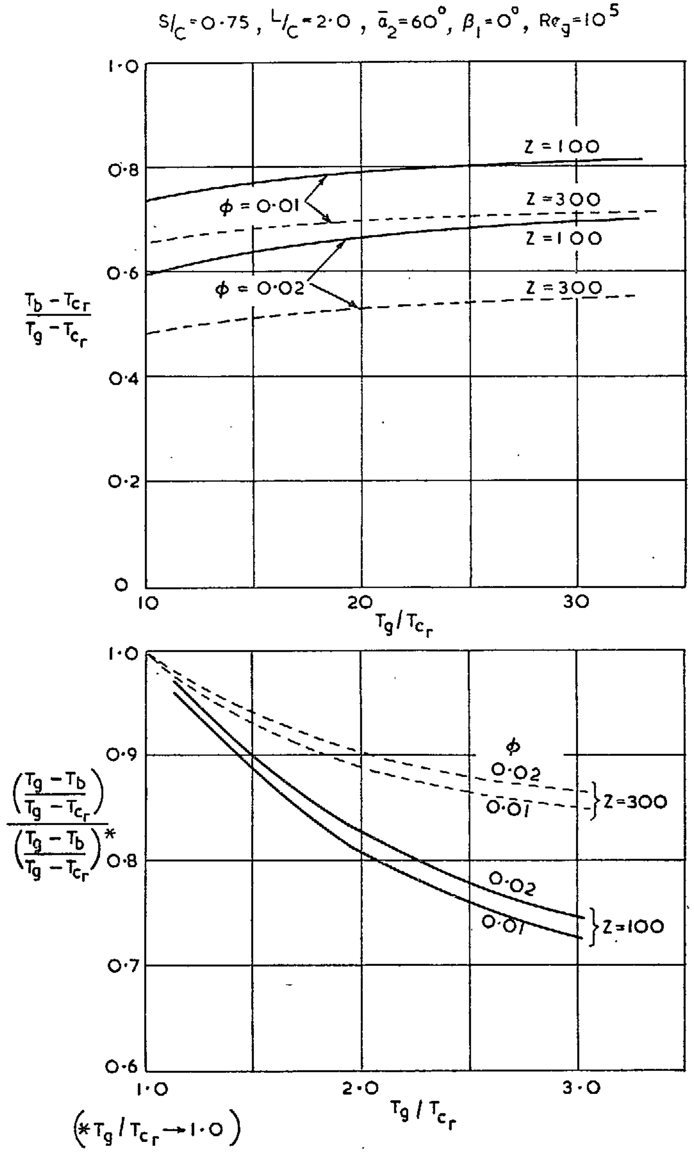

FIG. 8. Effect of temperature ratio T_g/T_{cr} on blade relative temperatures (l/L — 0·6).

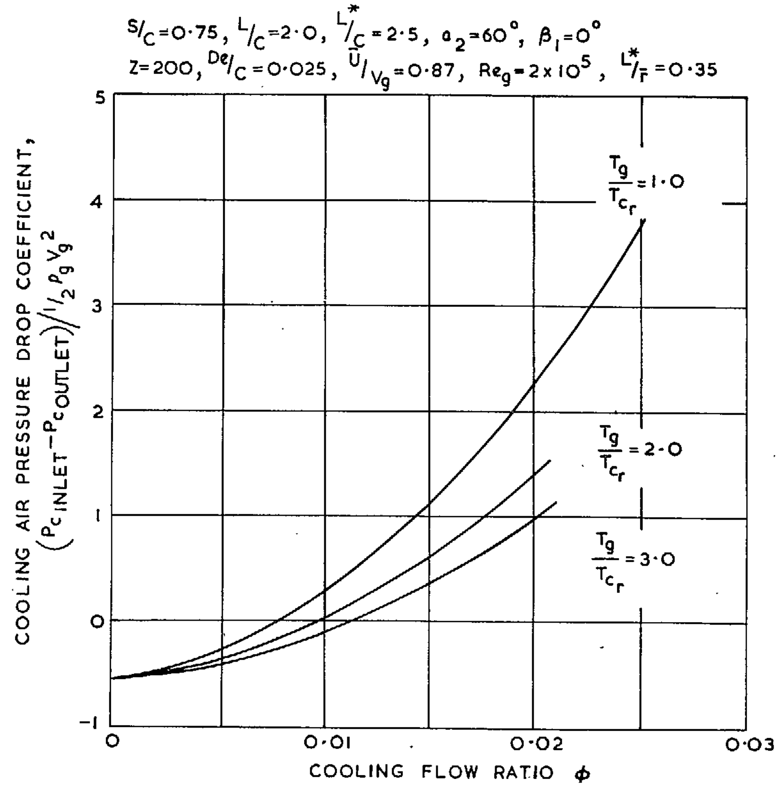

FIG. 9. Influence of temperature ratio on cooling-air pressure losses in reference blade.

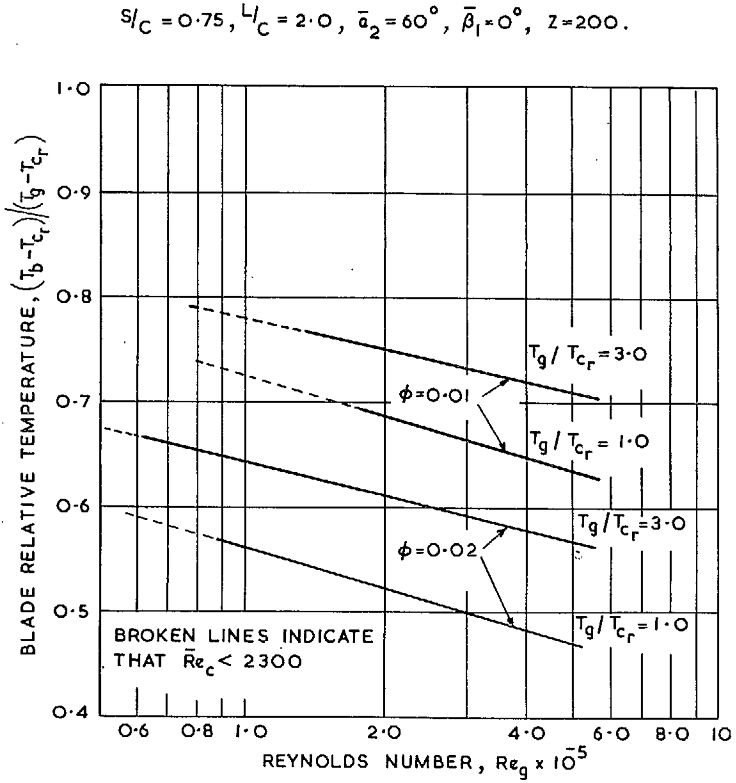

FIG. 10. Influence of Reynolds number on blade relative temperature.

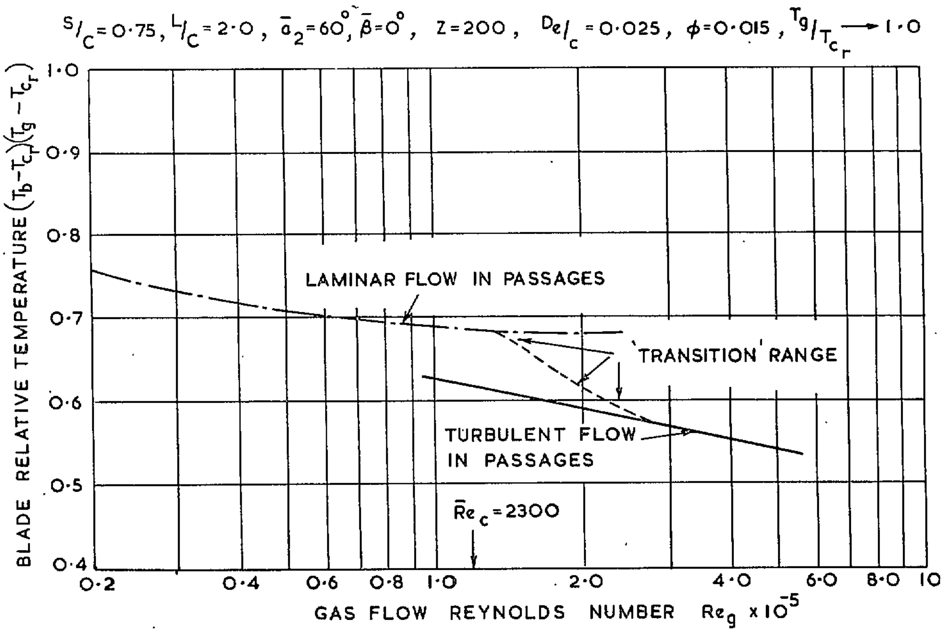

FIG. 11. Influence of gas-flow Reynolds number on blade relative temperatures of reference blade ($l/L = 0{\cdot}6$).

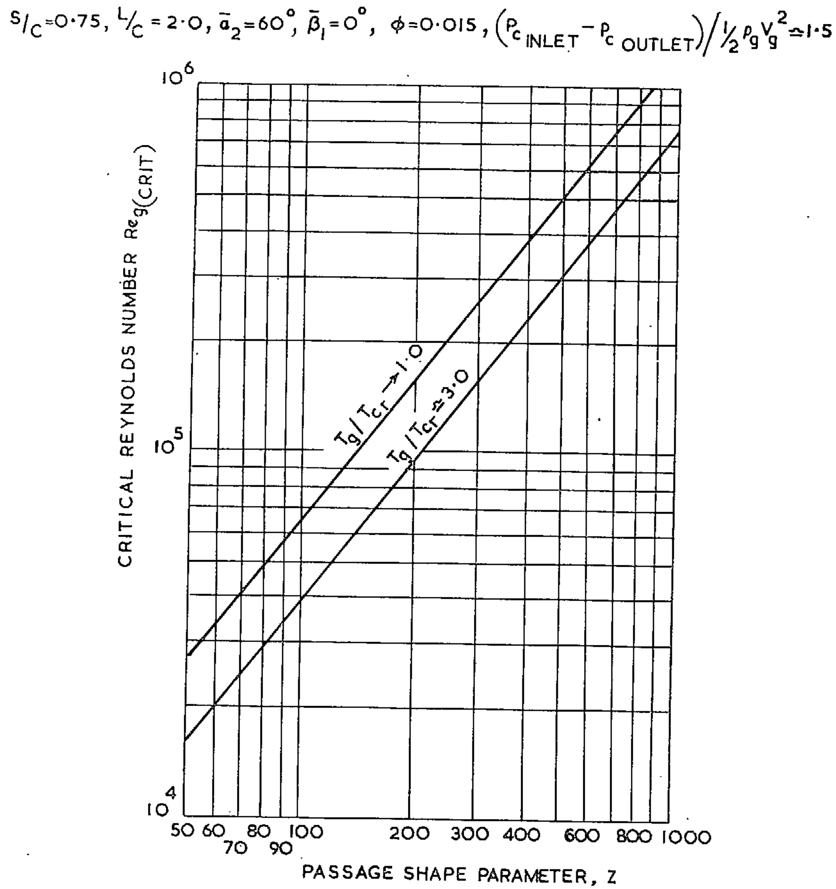

FIG. 12. Variation of minimum gas-flow Reynolds number for turbulent flow in the cooling passages of the reference blade.

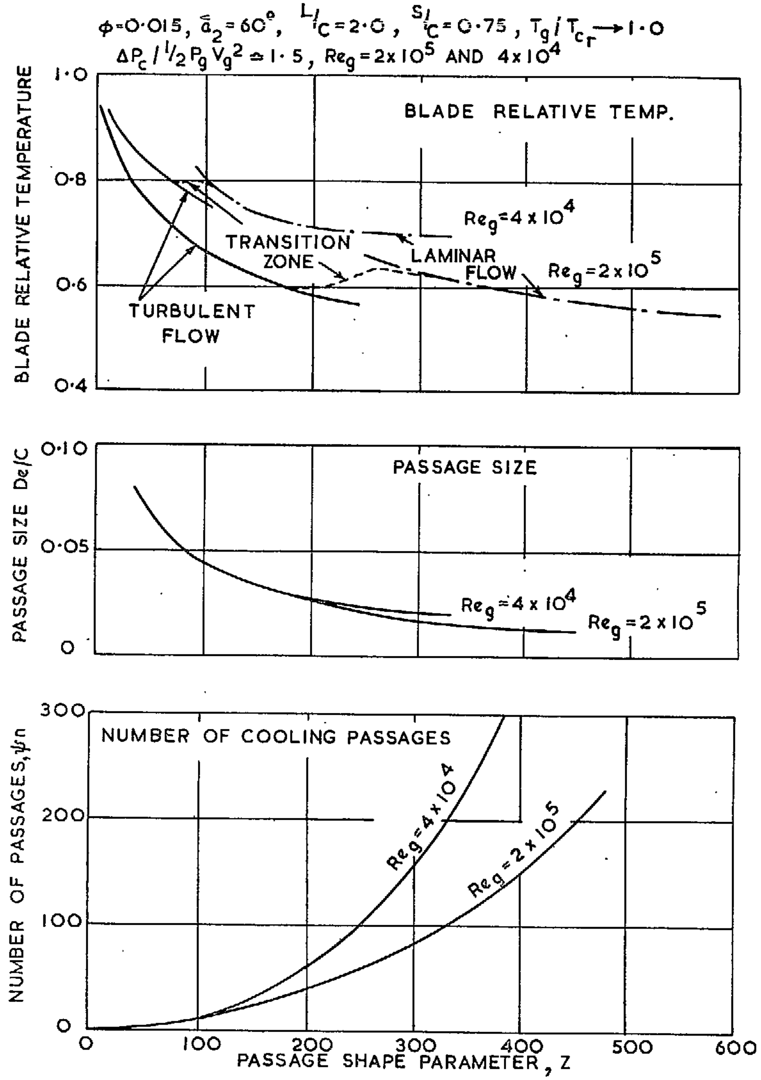

FIG. 13. Variation of blade relative temperature, cooling passage size and number of cooling passages with the value of the passage-shape parameter for turbulent-cooling and laminar-cooling flow (constant pressure drop).

(68094) Wt. 20/9036 K.7 8/57 Hw.

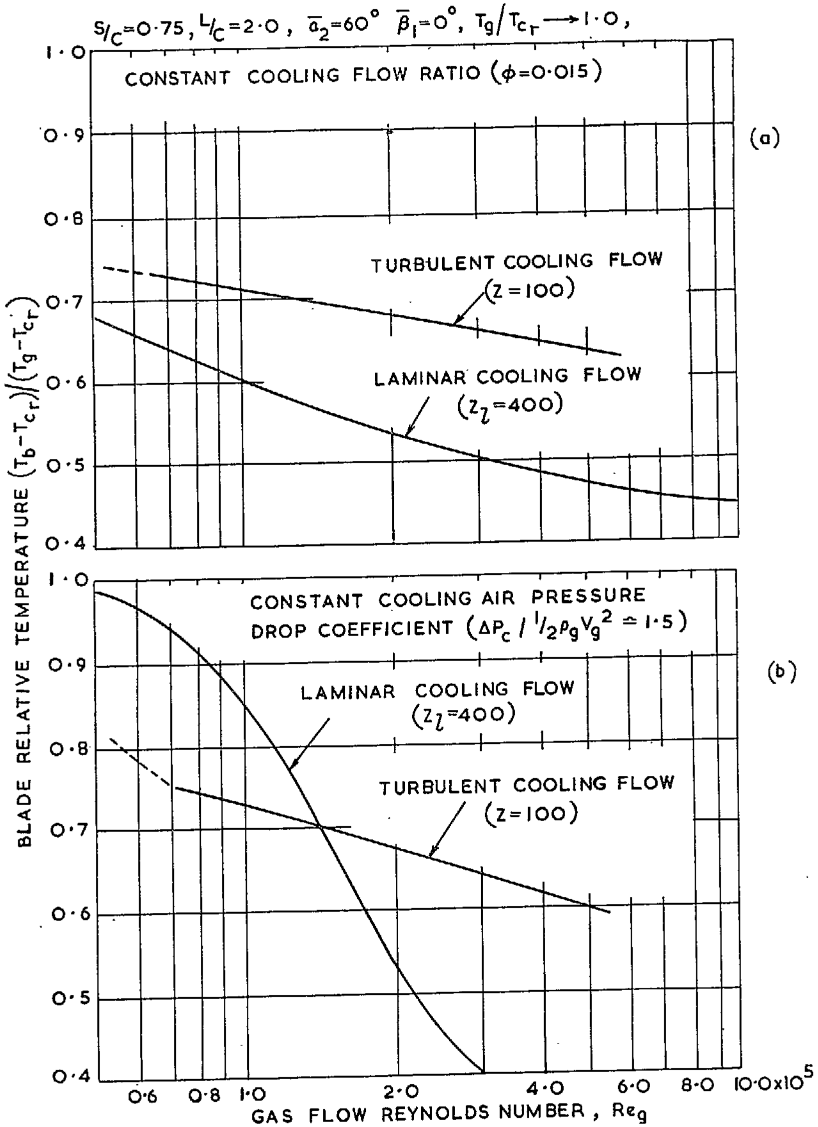

FIG. 14. Influence of gas-flow Reynolds number on blade relative temperature with laminar-cooling and turbulent-cooling flow.

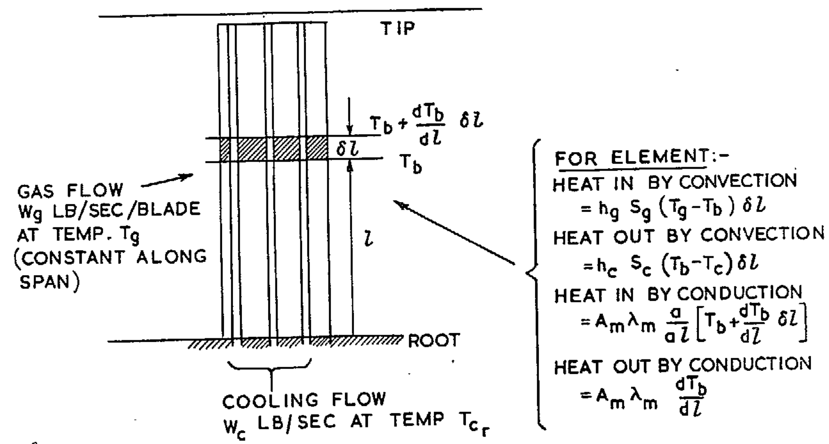

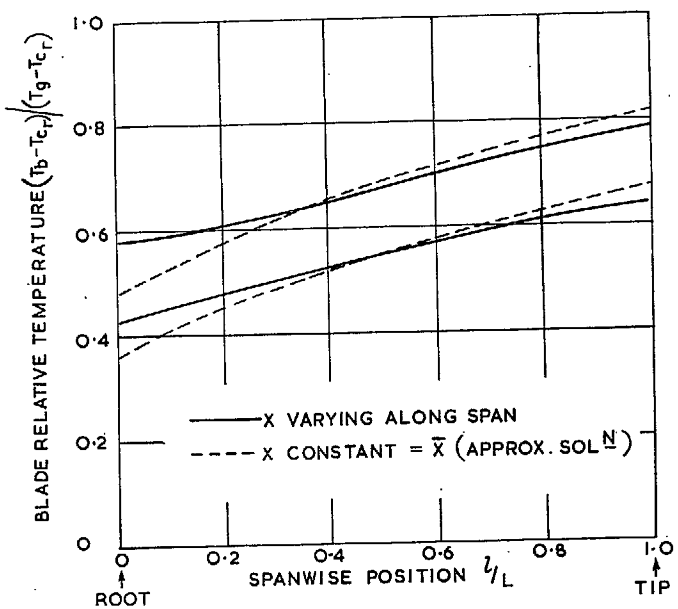

FIG. 15. Comparison of true and approximate solutions of equations for blade relative temperatures (Appendix I).

Publications of the Aeronautical Research Council

ANNUAL TECHNICAL REPORTS OF THE AERONAUTICAL RESEARCH COUNCIL (BOUND VOLUMES)

1939 Vol. I. Aerodynamics General, Performance, Airscrews, Engines. 50*s.* (51*s.* 9*d.*).
Vol. II. Stability and Control, Flutter and Vibration, Instruments, Structures, Seaplanes, etc. 63*s.* (64*s.* 9*d.*)

1940 Aero and Hydrodynamics, Aerofoils, Airscrews, Engines, Flutter, Icing, Stability and Control Structures, and a miscellaneous section. 50*s.* (51*s.* 9*d.*)

1941 Aero and Hydrodynamics, Aerofoils, Airscrews, Engines, Flutter, Stability and Control Structures. 63*s.* (64*s.* 9*d.*)

1942 Vol. I. Aero and Hydrodynamics, Aerofoils, Airscrews, Engines. 75*s.* (76*s.* 9*d.*)
Vol. II. Noise, Parachutes, Stability and Control, Structures, Vibration, Wind Tunnels. 47*s.* 6*d.* (49*s.* 3*d.*)

1943 Vol. I. Aerodynamics, Aerofoils, Airscrews. 80*s.* (81*s.* 9*d.*)
Vol. II. Engines, Flutter, Materials, Parachutes, Performance, Stability and Control, Structures. 90*s.* (92*s.* 6*d.*)

1944 Vol. I. Aero and Hydrodynamics, Aerofoils, Aircraft, Airscrews, Controls. 84*s.* (86*s.* 3*d.*)
Vol. II. Flutter and Vibration, Materials, Miscellaneous, Navigation, Parachutes, Performance, Plates and Panels, Stability, Structures, Test Equipment, Wind Tunnels. 84*s.* (86*s.* 3*d.*)

1945 Vol. I. Aero and Hydrodynamics, Aerofoils. 130*s.* (132*s.* 6*d.*)
Vol. II. Aircraft, Airscrews, Controls. 130*s.* (132*s.* 6*d.*)
Vol. III. Flutter and Vibration, Instruments, Miscellaneous, Parachutes, Plates and Panels, Propulsion. 130*s.* (132*s.* 3*d.*)
Vol. IV. Stability, Structures, Wind Tunnels, Wind Tunnel Technique. 130*s.* (132*s.* 3*d.*)

Annual Reports of the Aeronautical Research Council—

1937 2*s.* (2*s.* 2*d.*) 1938 1*s.* 6*d.* (1*s.* 8*d.*) 1939–48 3*s.* (3*s.* 3*d.*)

Index to all Reports and Memoranda published in the Annual Technical Reports, and separately—

April, 1950 - - - - R. & M. 2600 2*s.* 6*d.* (2*s.* 8*d.*)

Author Index to all Reports and Memoranda of the Aeronautical Research Council—

1909—January, 1954 R. & M. No. 2570 15*s.* (15*s.* 6*d.*)

Indexes to the Technical Reports of the Aeronautical Research Council—

December 1, 1936—June 30, 1939	R. & M. No. 1850	1*s.* 3*d.* (1*s.* 5*d.*)
July 1, 1939—June 30, 1945	R. & M. No. 1950	1*s.* (1*s.* 2*d.*)
July 1, 1945—June 30, 1946	R. & M. No. 2050	1*s.* (1*s.* 2*d.*)
July 1, 1946—December 31, 1946	R. & M. No. 2150	1*s.* 3*d.* (1*s.* 5*d.*)
January 1, 1947—June 30, 1947	R. & M. No. 2250	1*s.* 3*d.* (1*s.* 5*d.*)

Published Reports and Memoranda of the Aeronautical Research Council—

Between Nos. 2251–2349	R. & M. No. 2350	1*s.* 9*d.* (1*s.* 11*d.*)
Between Nos. 2351–2449	R. & M. No. 2450	2*s.* (2*s.* 2*d.*)
Between Nos. 2451–2549	R. & M. No. 2550	2*s.* 6*d.* (2*s.* 8*d.*)
Between Nos. 2551–2649	R. & M. No. 2650	2*s.* 6*d.* (2*s.* 8*d.*)

Prices in brackets include postage

HER MAJESTY'S STATIONERY OFFICE

York House, Kingsway, London, W.C.2; 423 Oxford Street, London, W.1; 13a Castle Street, Edinburgh 2; 39 King Street, Manchester 2; 2 Edmund Street, Birmingham 3; 109 St. Mary Street, Cardiff; Tower Lane, Bristol 1; 80 Chichester Street, Belfast, *or through any bookseller.*

S.O. Code No. 23-3013

R. & M. No. 3013